2023

A Gain-of-Function Role of Apolipoprotein E2 in Melanoma Progression

Nneoma Adaku

A GAIN-OF-FUNCTION ROLE OF APOLIPOPROTEIN E2 IN MELANOMA PROGRESSION

A Thesis Presented to the Faculty of
The Rockefeller University
in Partial Fulfillment of the Requirements for
the degree of Doctor of Philosophy

by
Nneoma Adaku
December 2022

A GAIN-OF-FUNCTION ROLE OF APOLIPOPROTEIN E2 IN MELANOMA PROGRESSION

Nneoma Adaku, Ph.D.
The Rockefeller University 2022

Genetic polymorphism of the secreted lipid transporter apolipoprotein E (APOE) plays important roles in the development of atherosclerosis and Alzheimer's disease. More recently, three common *APOE* alleles have been implicated as modulators of melanoma progression and survival. Melanoma patients born with a copy of the *APOE4* allele exhibit improved disease survival and responses to immunotherapy. Conversely, *APOE2* allele carriers experience substantially worsened survival outcomes compared to *APOE4* carriers and *APOE3* homozygotes. These survival differences are partly governed by effects on the immune system, as the *APOE4* genotype augments anti-tumor immunity. However, APOE variants also exert direct suppressive effects on melanoma cell metastatic behavior in an APOE4>APOE3>APOE2 order of potency. The molecular processes underlying the melanoma cell-intrinsic response to APOE variants are poorly characterized.

In this thesis I describe the generation and characterization of a genetically engineered mouse model for melanoma that expresses each of the human *APOE* alleles. I show that this autochthonous model closely recapitulates the *APOE2>APOE3>APOE4* order of melanoma progression observed in human patients. Transcriptomic analysis of tumors derived from this genetic model revealed upregulation of mRNA translation in *APOE2* melanomas relative to *APOE4*

melanomas. After experimental examination of the effects of APOE variants on melanoma translational efficiency, I report the discovery that APOE2 acts in a gain-of function manner to enhance pro-tumorigenic protein synthesis in melanoma cells. Melanoma cell-specific deletion of the APOE receptor LRP1 in the genetic mouse model abolished differences in tumor growth, metastasis, and protein synthesis between the *APOE2* and *APOE4* genotypes, thus revealing a melanoma cell-intrinsic APOE2/LRP1 axis that serves to promote melanoma progression. Analysis of a melanoma patient RNA-Seq dataset demonstrated upregulation of mRNA translation processes in *APOE2* patient tumors, thus providing clinical relevance for these findings. Altogether, this thesis identifies a potentially therapeutically targetable pathway in melanoma and reveals a novel gain-of-function role of the *APOE2* allele, which may have implications for other diseases impacted by *APOE* genetics.

I am who I am, doing what I came to do

– Audre Lorde

Aki ga-agba mmanụ aghaghị igabiga n'ọkụ

ACKNOWLEDGEMENTS

Many individuals helped make this thesis possible. I'd first like to thank my PhD advisor Sohail Tavazoie for providing the guidance, generous resources, independence, and supportive community of lab colleagues that enabled me to grow into the confident scientist that I am today. I am grateful towards my fellow Tavazoie Lab members for always being available for advice and providing thoughtful feedback on my work over the years. I am especially grateful to alum Benjamin Ostendorf for his excellent mentorship when I first started in the lab and for providing such a strong foundation for me to follow up on his APOE variant discoveries. Similarly, though we have never met, I'd like to thank alum Nora Pencheva for starting the APOE project in the lab and performing such outstanding work that it made my subsequent studies much easier to perform. I thank Jess Posada for her vital pathology expertise. I also thank recent MD-PhD lab alumni Maria Passarelli, Lisa Earnest-Noble, and Doowon Huh for charting a path for my success.

I am immensely grateful to my thesis committee members Ping Chi, Paul Cohen, and Sid Strickland for their support, kindness, advice, and useful feedback as this thesis work developed. I can genuinely say our meetings were among the high points of my PhD. I would also like to thank my external examiner Theresa Vincent for generously providing her time and expertise. I'm appreciative of all the members of the Tri-Institutional MD-PhD Program Office and the Rockefeller Dean's Office for providing the institutional structure and support that enabled me to thrive.

I also thank other members of the Rockefeller community for helping make this all possible in various ways: Vaughn Francis and fellow staff of the Comparative Bioscience Center for their indispensable maintenance of my mouse colony, Alison Ashbrook of the Rice laboratory, members of the Rockefeller Inclusive Science Initiative, the Bass Dining Hall staff, Soren Heissel and Henrik Molina of the Proteomics Resource Center, and members of the Research Restart Committee/RUStrong staff for enabling me to stay healthy and productive despite working through the COVID-19 pandemic for the majority of my PhD.

Finally, to my MD-PhD entering class of 2016 cohort for being a fun and supportive group of people to go through this experience with. To my friends that I had at the outset of this journey and to those that I've made along the way. To Zuri for always keeping me grounded. And to my feline companions Benji and Basqui.

TABLE OF CONTENTS

LIST OF FIGURES

LIST OF ABBREVIATIONS

4-OHT 4-hydroxytamoxifen
APOE ..... apolipoprotein E
BPC ..... *Braf$^{V600E/+}$;Pten$^{-/-}$;Tyr::CreER*
AKT ..... AKT serine/threonine kinase
BRAF ..... B-Raf proto-oncogene, serine/threonine kinase
CDKN2A ..... cyclin-dependent kinase inhibitor 2A
CHX ..... cycloheximide
CRISPR ..... clustered regularly interspaced short palindromic repeats
CTLA-4 ..... cytotoxic T-lymphocyte associated protein 4
ERK ..... extracellular signal-regulated kinase
FDA ..... Food and Drug Administration
GEMM ..... genetically engineered mouse model
GFP ..... green fluorescent protein
GSEA ..... gene set enrichment analysis
H&E ..... hematoxylin and eosin
HDL ..... high-density lipoprotein
IFN ..... interferon
IL ..... interleukin
kDa ..... kilodalton
LDL ..... low-density lipoprotein
LDLR ..... low-density lipoprotein receptor
LRP1 ..... low density lipoprotein receptor-related protein 1
LRP1B ..... low density lipoprotein receptor-related protein 1B
LRP8 ..... low density lipoprotein receptor-related protein 8
MAPK ..... mitogen-activated protein kinase
MEK ..... MAPK/ERK kinase
mTOR ..... mammalian target of rapamycin
NMR ..... nuclear magnetic resonance
PD-1 ..... programmed cell death protein 1
PD-L1 ..... programmed death-ligand 1
PDGF ..... platelet-derived growth factor
PI3K ..... phosphoinositide 3-kinase
PTEN ..... phosphatase and tensin homolog
RNA-Seq ..... RNA sequencing
SKCM ..... skin cutaneous melanoma
SUnSET ..... surface sensing of translation
TCGA ..... The Cancer Genome Atlas
TGFb ..... transforming growth factor beta
TR ..... triple reporter
VLDL ..... very-low-density lipoprotein
VLDLR ..... very-low-density lipoprotein receptor
WES ..... whole exome sequencing

CHAPTER 1. INTRODUCTION

Melanoma is a cancer caused by the malignant transformation of melanocytes, the pigment-producing cells of the body. Melanoma represents only approximately 4% of all skin cancers. Other skin cancers include basal cell and squamous cell carcinomas, which are among the most commonly diagnosed malignancies in the world. Despite its relative rarity among dermatological cancers, melanoma is responsible for upwards of 80 percent of all skin cancer deaths (Miller and Mihm, 2006). This is due to its propensity to form distant metastases. Patients diagnosed with localized disease have a 5-year survival rate of 99% and are considered cured after excision of the skin lesion. The 5-year survival rate of patients diagnosed with distant disease, however, drops precipitously to just 30% (Surveillance Research Program, 2022). Thus, there remains a great need to understand the biological contributors to melanoma metastatic progression for melanoma to become a manageable disease like most other skin cancers.

1.1 Epidemiology of melanoma

In 2022 approximately 100,000 individuals in the United States will have been diagnosed with melanoma, accompanied by nearly 8000 deaths (American Cancer Society, 2022). The incidence of melanoma has increased dramatically over the past few decades, particularly among men who experienced a 17-fold increase of incidence from 1.9 cases per 100,000 in the 1950s to 33.5 in 2007 (Geller et al., 2013). The rate of melanoma death has not increased as dramatically, however,

raising the question of whether this increase in incidence can be primarily attributed to overdiagnosis (Glasziou et al., 2020; Welch et al., 2021).

The primary modifiable risk factor for development of cutaneous melanoma, the focus of this thesis, is ultraviolet light exposure, as UV radiation causes bulky pyrimidine dimers that can lead to DNA damage and ultimately carcinogenesis (Saginala et al., 2021). Thus eumelanin, which is produced in greater quantities in darker-skinned individuals, is the major protective factor against melanoma development because of its efficient dissipation of UV radiation in the skin. This UV and melanin dependence causes substantial geographic and racial/ethnic distributions in melanoma risk. Melanoma risk increases with proximity to the Equator, due to higher sun exposure, and European ancestry, due to lighter skin (Matthews et al., 2017). The confluence of these two factors can be observed in white populations in northern Australia and New Zealand, who have the highest rates of melanoma incidence in the world (Matthews et al., 2017).

1.2 Molecular contributors to melanoma

Melanoma is characterized by a variety of driver mutations that occur with high frequency in patient tumors. The most common activating mutation in melanoma is a substitution from valine to glutamate at the 600 position of the BRAF protein (BRAF V600E). BRAF is an upstream kinase in the MAPK/ERK pathway, thus its constitutive activation leads to enhanced cellular proliferation and survival (Davis et al., 2018). BRAF mutations occur in over 60% of cutaneous melanomas, as well as

up to 80% of benign nevi, or moles. However, most nevi do not progress to melanoma, and BRAF V600E actually leads to oncogene-induced senescence in melanocytes (Michaloglou et al., 2005). This suggests the necessity of additional mutations for progression to malignancy. Indeed, nearly half of BRAF-mutant tumors also possess a disruptive alteration in the *PTEN* tumor suppressor gene, which leads to activation of the PI3 kinase/AKT signaling pathway (Hodis et al., 2012). This combination leads to highly penetrant, highly invasive melanoma formation in mice (Dankort et al., 2009). Mutations in NRAS are the second most common activating mutations in melanoma, occurring in over 20% of tumors (Davis *et al.*, 2018). As NRAS is upstream of both the MAPK/ERK and AKT/mTOR signaling pathways, activating mutations also lead to cell growth, proliferation, and survival. These mutations exist in a mutually exclusive manner from BRAF mutations (Hodis et al., 2012). Furthermore, up to 10% of melanomas are the result of familial syndromes (Rossi et al., 2019). The most commonly altered gene in familial melanoma is *CDKN2A*, which is mutated in upwards of 40% cases. *CDKN2A* is a tumor suppressor gene that acts upstream of the Rb, CDK4, and p53 pathways to regulate cell cycle progression and apoptosis. Due to the potent effect of its inactivation, approximately 69% of sporadic melanomas also possess an alteration in CDKN2A (Cancer Genome Atlas Network, 2015).

1.3 Melanoma metastatic cascade

Metastasis has been viewed a stepwise process that tumor cells must undertake in order to progress from the primary to metastatic site. This “metastatic cascade” involves: 1) the recruitment of blood vessels to the primary tumor via angiogenesis 2) invasion into the local stroma 3) intravasation into and circulation through the vasculature 4) arrest at a distant site and extravasation into the tissue and 5) proliferative colonization of the distant site (Talmadge and Fidler, 2010). This process is incredibly inefficient. Though an estimated 1 million cells are shed into the vasculature per gram of tumor per day, less than 0.01% of tumor cells are estimated to complete all steps needed to become a metastatic tumor (Butler and Gullino, 1975; Fidler, 1970). The later process of colonization has been identified as the predominant rate-limiting step of metastasis (Damsky et al., 2014; Luzzi et al., 1998).

In melanoma, the metastatic cascade has largely been represented using the Clark model, which was first proposed in 1984. Under this model, melanoma progresses in the following order: 1) a benign melanocytic nevus 2) a dysplastic nevus with cellular atypia 3) the radial growth phase in which melanoma cells spread laterally 4) the vertical growth phase during which dermal invasion occurs and finally 5) metastasis (Clark et al., 1984) **(Figure 1.1)**. However, this linear order has been challenged in recent years, as it has been histologically observed in only a third of melanoma cases (Balch et al., 2020) and recent evidence suggests that melanoma cells can metastasize even before a clinically identifiable primary tumor has formed (Damsky et al., 2014).

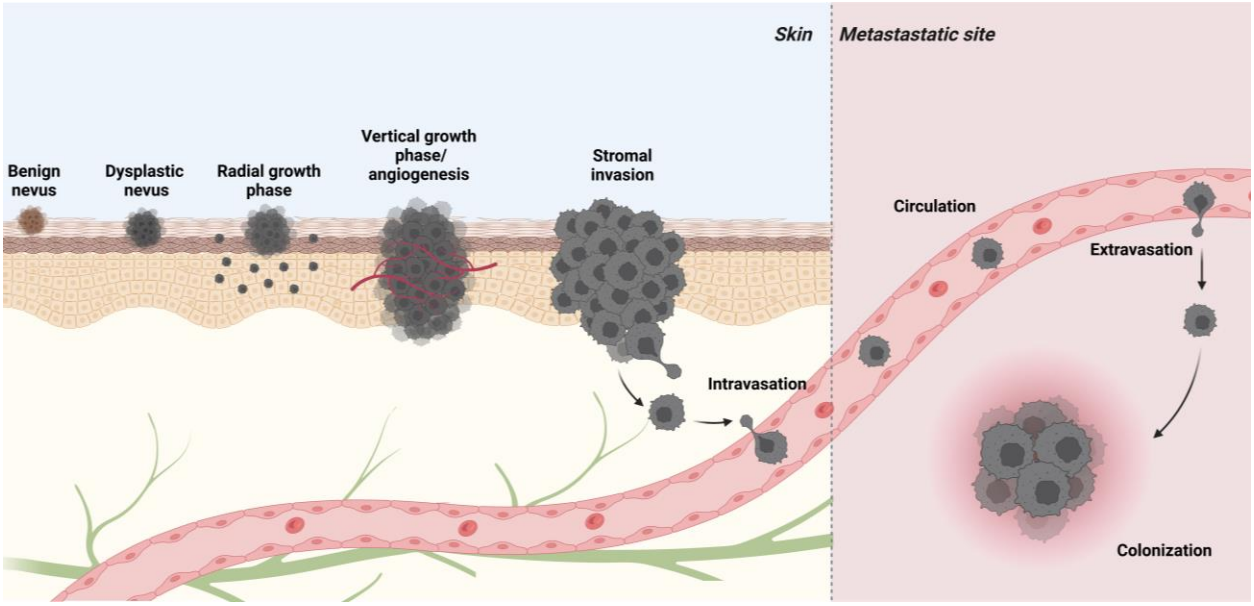

Figure 1.1 Melanoma metastatic cascade. Integrated representation of the Clark model and the metastatic cascade. Under the Clark model, melanomas progress from a benign nevus, to a dysplastic nevus, to the radial growth phase with lateral spread, to the vertical growth phase with dermal invasion, and then to a metastatic tumor. During metastasis, cancer cells intravasate into the bloodstream, survive in the circulation, extravasate at a distant site, and colonize the new metastatic niche.

Tumors often have a predilection for what organs they metastasize to. This observation was made over a century ago by surgeon Stephen Paget, who coined the “seed and soil” hypothesis. This hypothesis posits that certain organ environments (soil) are more hospitable to certain cancer cells (seeds) (Paget, 1889). Indeed, melanoma has a propensity to spread to the lung (18-36% of patients with metastasis), liver (~20%), brain (~20%), and bone (~17%) (Balch et al., 2020). Though one could speculate that much of this organotropism is attributable to the large amount of blood flow that these organs receive, modeling approaches suggest that blood flow accounts for ≤1% of metastasis to the liver, lung, or brain (Font-Clos et al., 2020). Furthermore, metastasis to organs such as the heart and kidney is rare

despite their high levels of perfusion. In addition to cancer cell-intrinsic properties such as chemokine receptor expression that may modulate melanoma organotropism, mounting evidence suggests that melanoma cells are capable of secreting factors that generate a hospitable premetastatic niche in the target organ, as opposed to the metastatic site simply being inherently conducive to colonization (Damsky et al., 2010; Kaplan et al., 2005; Peinado et al., 2017). Thus, metastasis represents a complex, bidirectional interplay between cancer cells and the metastatic niche.

The determinants of metastatic competency remain elusive. It is now well known that tumors consist of a heterogenous population of cells with inherently different metastatic capacities, and a process of evolutionary selection occurs during metastatic progression (Talmadge and Fidler, 2010). Much effort has been taken to identify somatic mutations that make a primary tumor cell become a metastatic one in a similar manner to the many mutations that are known to drive tumorigenesis. However, genetic alterations found in metastatic tumors are mostly shared with the original primary tumor (Vogelstein et al., 2013). Furthermore, the few potential metastasis-driving mutations identified in melanoma have yet to reach a scientific consensus (Turner et al., 2018). Instead, non-mutational processes such as phenotypic plasticity, dormancy, and metabolic rewiring are increasingly being implicated (Celia-Terrassa and Kang, 2016; Rambow et al., 2019).

1.4 Therapeutic interventions in melanoma

1.4.1 Targeted therapy

The identification of the MAPK signaling pathway as a major oncogenic driver in melanoma led to the search for molecules that could therapeutically target its activity. The first of these molecules was vemurafenib, a selective BRAF V600E inhibitor that was approved by the FDA in 2011 for the treatment of unresectable and metastatic BRAF V600E-positive melanomas (Domingues et al., 2018). This was a major advancement in melanoma treatment, causing tumor regression in upwards of 90% of patients. Similar MAPK pathway inhibitors were subsequently approved, all within just the past decade, including the additional BRAF inhibitors dabrafenib and encorafenib and the MEK inhibitors trametinib, cobimetinib, and binimetinib. BRAF and MEK inhibitors are often given in combination, providing even more potent MAPK signaling suppression. However, as has been the limitation for targeted therapies in other cancer types, tumors often relapse due to the development of escape mutations that reactivate the MAPK pathway or compensate for its absence. Thus, the median progression-free survival on BRAF/MEK combination therapy remains at approximately one year (Balch et al., 2020).

1.4.2 Immunotherapy

Immunotherapy has been a mainstay of melanoma treatment since the 1990s. High-dose treatments with the cytokines IFNα-2b and IL-2 were FDA approved in

1995 and 1998, respectively, as a method to stimulate anti-tumor immune cell activity (Domingues et al., 2018). However, both treatments had modest efficacy with a high rate of severe adverse events. A major breakthrough occurred with the discovery of immune checkpoint blockade, which involves using antibodies to block inhibitory molecules that serve to rein in T cell activity. The first of these antibodies was ipilimumab, which was approved in 2011. Ipilimumab targets CTLA-4, a receptor on the surface of T cells whose activation leads to the inhibition of T cell proliferation and activation (Balch et al., 2020). Thus CTLA-4 blockade leads to anti-tumor T cell expansion, infiltration, and cytokine production. This was followed by the approvals of nivolumab (2014) and pembrolizumab (2015) which bind to PD-1, another T cell inhibitory molecule. Its ligand PD-L1 is often highly expressed by cancer cells as a mechanism of immune evasion (Balch et al., 2020). Anti-PD-1 antibodies cause more durable patient responses and less severe toxicity compared to anti-CTLA-4, which quickly made them the standard of care for immunotherapy. Altogether, the recent advent of targeted molecules and immunotherapy has revolutionized melanoma treatment, leading to an increase in 5-year survival for metastatic patients from 17% in 2004 to 33% just 15 years later (Surveillance Research Program, 2022). This, however, still leaves much room for the discovery of new therapeutically targetable mechanisms of melanoma progression.

1.5 Biology of apolipoprotein E

1.5.1 Canonical and non-canonical roles of APOE

Apolipoprotein E (APOE) is a 34 kDa secreted glycoprotein that was initially discovered in the early 1970s as a protein component of very low density lipoprotein (VLDL), the predominant triglyceride transport particle in the plasma (Shore and Shore, 1973). As such, the canonical role of APOE is to mediate lipid metabolism. The liver accounts for over 75% of APOE production, where it is incorporated into liver-secreted VLDL particles that go on to be hydrolyzed by lipoprotein lipase into fatty acids as an energy source for extrahepatic cells. APOE also mediates dietary lipid metabolism, as it is incorporated into chylomicron remnants after their secretion by the small intestine. These chylomicrons can go on to be hydrolyzed for energy similarly to VLDL or be transported to the liver for excretion into the bile. APOE can also mediate cholesterol efflux from cells in a process called reverse cholesterol transport. High-density lipoprotein (HDL) particles serve as cholesterol acceptors, which, when complexed with APOE, can deliver excess cellular cholesterol to the liver (Mahley and Rall, 2000). For these reasons, APOE is a major regulator of plasma lipid levels and cardiovascular disease risk. Plasma triglyceride levels vary according to plasma APOE level (Salah et al., 1997), and *Apoe* knockout mice display dramatically increased lipid levels and are highly prone to developing atherosclerotic lesions even on a normal chow diet (Nakashima et al., 1994).

Macrophages are a major extra-hepatic source of APOE, which further implicates APOE as a modulator of atherosclerosis development as well as inflammation and immune system function. APOE secreted by macrophages in the arterial wall helps prevent plaque formation by inhibiting lipid oxidation, vascular smooth muscle cell proliferation, platelet aggregation, and foam cell generation via its facilitation of reverse cholesterol transport (Martinez-Martinez et al., 2020). APOE may also promote an anti-inflammatory macrophage phenotype and regulate bone marrow monocyte production (Kockx et al., 2018). In addition to its effects on innate immune cells, APOE has been shown to inhibit T cell proliferation and mediate susceptibility to numerous infections including herpes simplex virus, human immunodeficiency virus, *Listeria monocytogenes*, and malaria (Mahley and Rall, 2000).

The central nervous system is the other major site of APOE production. Here, APOE serves as the primary apolipoprotein. The brain is the most cholesterol-rich organ in the body and its cholesterol metabolism is compartmentalized, thus giving APOE major implications for brain function (Mahley, 2016). Astrocytes are the predominant producers of APOE in the brain, though neurons have been shown to produce APOE upon injury (Xu et al., 2006). The formation of HDL-like particles by APOE helps redistribute cholesterol among cells in the brain, where it serves crucial roles in myelination, membrane remodeling, synaptogenesis, and neuronal repair (Mahley, 2016). APOE also has direct roles in modulating neurite outgrowth and

amyloid β clearance (Mahley and Rall, 2000). In sum, APOE has varied, pleiotropic functions in mammalian biology.

1.5.2 APOE receptor biology

The cholesterol influx and efflux processes regulated by APOE are both mediated by the presence of APOE receptors on target cells. These receptors, which include LDLR, LRP1, VLDLR, LRP8, and LRP1B, among others, are members of the large, highly conserved low-density lipoprotein (LDL) receptor family. All core members contain a large extracellular domain that binds APOE and a variety of other ligands, a transmembrane domain, and an intracellular domain containing NPXY tyrosine phosphorylation motifs that mediate signal transduction and endocytic trafficking (Lane-Donovan and Herz, 2017). LDLR, the first identified member of the family, is ubiquitously expressed and is the predominant lipoprotein acceptor. As such, deficiencies in LDLR function cause severe hypercholesterolemia. APOE is a highly efficient ligand for LDLR, thus making APOE the major facilitator of receptor-mediated clearance of VLDL and chylomicron remnants (Mahley and Huang, 1999).

Low density lipoprotein receptor-related protein 1 (LRP1) was the second characterized APOE receptor due to the observation that chylomicron remnant uptake was unaffected in the absence of LDLR. This finding was followed by the identification of an LDLR-like receptor that was highly expressed in the liver (Herz et al., 1988; Mahley and Huang, 1999). LRP1 exists at the cell surface of all cell types,

particularly hepatocytes and neurons, as a large 515 kDa extracellular ligand binding domain and an 85 kDa cytoplasmic domain. In addition to APOE, it has been shown to bind at least 40 other ligands. This confers it diverse roles in processes other than chylomicron remnant uptake, including endocytic clearance, extracellular matrix organization, coagulation, cell migration, viral entry, and maintenance of vascular integrity (Herz and Strickland, 2001; Lillis et al., 2008). The cytoplasmic tyrosine phosphorylation domain of LRP1 also makes it a major hub for signaling pathways due to its ability to bind a variety of adaptor proteins (Guttman et al., 2009; Van Gool et al., 2015). These include growth factor signaling pathways that are of relevance to cancer, such as the PDGF, TGFb, MAPK, and PI3K/AKT pathways (Boucher and Herz, 2011; Muratoglu et al., 2010). Indeed, LRP1 has frequently been implicated as a mediator of cancer progression, though whether it serves as a cancer promoter or inhibitor varies widely by study and cancer type (Boulagnon-Rombi et al., 2018; Dedieu et al., 2008; Fayard et al., 2009; Gonias and Campana, 2014; Langlois et al., 2010; Montel et al., 2007; Salama et al., 2018; Song et al., 2009; Van Gool et al., 2015). Its diversity of ligands and cellular functions means that the role of LRP1 in cancer is likely highly contextual.

1.5.3 Genetic variation in *APOE*

APOE exhibits physiologically significant genetic variation within the human population. There are three common alleles of the *APOE* gene, termed *APOE2*, *APOE3*, and *APOE4*. These alleles differ from each other at just two amino acid

positions, residues 112 and 158 (Belloy et al., 2019). APOE4, which is thought to be the ancestral allele from which the other two variants were derived, exhibits an arginine at both positions. APOE2, the youngest variant, has a cysteine at both positions, whilst APOE3 has a cysteine at position 112 and an arginine at position 158 **(Figure 1.2)**. These subtle amino acid substitutions lead to dramatic changes in APOE structure and binding. The presence of cysteine 158 in APOE2 alters the charge of its receptor binding domain, causing it to have less than 2% LDLR binding affinity compared to APOE3 and APOE4 (Schneider et al., 1981; Weisgraber et al., 1982). In contrast, the presence of arginine 112 in APOE4 causes the formation of a salt bridge between the protein's C and N terminal domains, leading to a compacted structure and alteration of its lipid binding region. This results in slightly enhanced LDLR affinity compared to APOE3 as well as a preference in binding VLDL rather than HDL (Bohnet et al., 1996; Knouff et al., 1999). In mice and non-human primates the structure and function of APOE most closely resembles APOE3, despite the APOE4-like presence of arginine at position 112 (Mahley et al., 2009). As a likely consequence of differences in binding affinity, it has been shown that APOE activates neuronal signaling downstream of APOE receptors in an APOE4>APOE3>APOE2 order of potency (Huang et al., 2019; Huang et al., 2017).

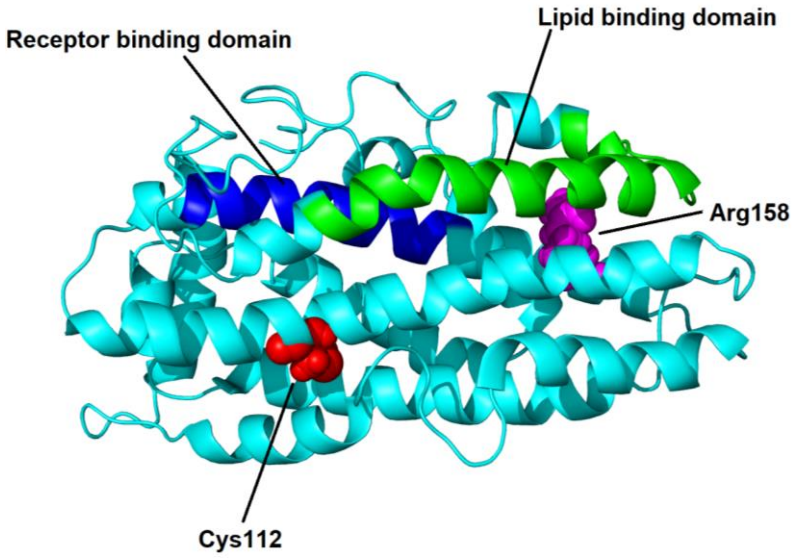

Figure 1.2 Structure of APOE3. NMR structure of APOE3 adapted from (Chen et al., 2011). Highlighted in red is cysteine 112, which is mutated to an arginine in APOE4. Highlighted in magenta is arginine 158, which is mutated to a cysteine in APOE2. Highlighted in green and blue are the lipid binding and receptor binding domains, respectively.

The frequency of each *APOE* allele varies greatly by geographical location. *APOE3* is the most common variant in the human population, ranging from as low as 69% in Africa to 85% in Asia (Belloy et al., 2019). *APOE4* has the most variable distribution, ranging from as low as 5% in the Mediterranean to 40% in Central Africa. *APOE2* shows little geographic variation with an overall allele frequency of about 7%, though it is completely absent in many groups that are indigenous to the Americas (Corbo and Scacchi, 1999). The geographic variation of *APOE* allele frequencies suggests that certain variants may have conferred evolutionary adaptations to location-specific challenges such as infection and nutrient deprivation (Huebbe and Rimbach, 2017). Among individuals of predominantly European ancestry, who experience the highest melanoma incidence, approximately

16% are *APOE2* carriers, 26% are *APOE4* carriers, and 61% are *APOE3* homozygotes (3% possess an *APOE2;APOE4* genotype) (Farrer et al., 1997).

The structural and functional differences between APOE variants have led to significant implications for human disease. Due to its role in lipid transport, *APOE* genetic variation has a major impact on cardiovascular disease risk. As a consequence of its poor LDLR binding, *APOE2* homozygotes are prone to developing type III hyperlipoproteinemia, a lipid disorder that leads to severe hyperlipidemia and early onset coronary artery disease (Mahley and Rall, 2000). Aside from this rare disorder, APOE2 is generally protective against cardiovascular disease, as the risk of developing coronary artery disease and myocardial infarction follows an *APOE4>APOE3>APOE2* pattern (Belloy *et al.*, 2019). *APOE4* is the strongest genetic risk factor for developing Alzheimer's disease. Carrying one *APOE4* allele doubles to quadruples one's risk of developing Alzheimer's, while carrying two alleles increases the risk 8 to 12-fold (Farrer *et al.*, 1997). This association is weak among African cohorts despite their high *APOE4* allele frequency, suggesting additional genetic and environmental contributors to the Alzheimer's risk (Belloy *et al.*, 2019). In contrast, *APOE2* is protective against Alzheimer's development (Corder et al., 1994). GWAS studies have also implicated *APOE* genotype as a modifier of longevity, with lifespan following an *APOE2>APOE3>APOE4* pattern (Belloy et al., 2019).

In the past 30 years, tens of thousands of studies have been performed to identify the molecular basis for Alzheimer's risk modification by *APOE* genotype.

Much of this work has benefitted from the development of *APOE*-targeted replacement (knock-in) mice, whose murine *Apoe* locus was replaced by one of the three human variants (Knouff *et al.*, 1999; Sullivan et al., 1997; Sullivan et al., 1998). As a consequence of the pleiotropic behavior of APOE, numerous mechanistic contributors have been identified for APOE4, including diminished amyloid beta clearance, decreased CSF APOE levels, impaired neuronal repair, mitochondrial dysfunction, cytoskeleton disruption, compromised blood-brain barrier integrity, and increased inflammation (Belloy *et al.*, 2019; Huang and Mahley, 2014). However, a decisive, therapeutically intervenable mechanism has remained elusive. Even less is known about the mechanisms behind the protective role of APOE2, as most studies have focused on comparing the effects of APOE3 and APOE4 (Suri et al., 2013). It has been debated whether the alleles simply represent a progressive loss of function of APOE from *APOE2* through to *APOE4*, or whether *APOE4* is a toxic gain-of-function allele. This is complicated by the fact that while Alzheimer's and atherosclerosis follow an *APOE4>APOE3>APOE2* risk order, other conditions such as hypertriglyceridemia and hemorrhagic stroke follow a U-shaped *APOE4>APOE3<APOE2* pattern (Belloy *et al.*, 2019). This inherent complexity of APOE leaves much to be discovered about its impacts on human disease despite its identification nearly 50 years ago.

1.5.4 Role of APOE in melanoma

More recently, APOE has been implicated as a suppressor of melanoma progression. As they become highly metastatic, melanoma cells upregulate a set of microRNAs that coordinately repress endogenous APOE expression (Pencheva et al., 2012). This leads to reduced APOE protein secretion from melanoma cells. Secreted APOE acts via LRP1 expressed on the surface of melanoma cells to inhibit their invasive capacity. Thus, its reduced secretion causes enhanced invasiveness and metastasis **(Figure 1.3)**. Additionally, APOE has cell-extrinsic roles in the tumor microenvironment. APOE inhibits the migration of endothelial cells by interacting with LRP8, thus repressing tumor angiogenesis. APOE also acts on LRP8 receptors expressed on immunosuppressive myeloid-derived suppressor cells to drive their apoptosis, thus enhancing anti-tumor immunity (Tavazoie et al., 2018). Melanoma-derived APOE serves to primarily affect metastatic capacity, as melanoma-specific *APOE* knockdown enhances metastasis but has no influence on primary tumor growth. In contrast, stromal APOE potently suppresses both primary and metastatic melanoma progression (Pencheva et al., 2014). This enabled the use of liver-X-receptor agonists as a therapeutic intervention in melanoma because they stimulate transcriptional activation of *APOE* in the tissues, thus enhancing melanoma suppression (Pencheva *et al.*, 2014). miRNA-mediated targeting of *APOE* is a significant example of how cancer cells can acquire metastatic fitness in the absence of additional somatic mutations.

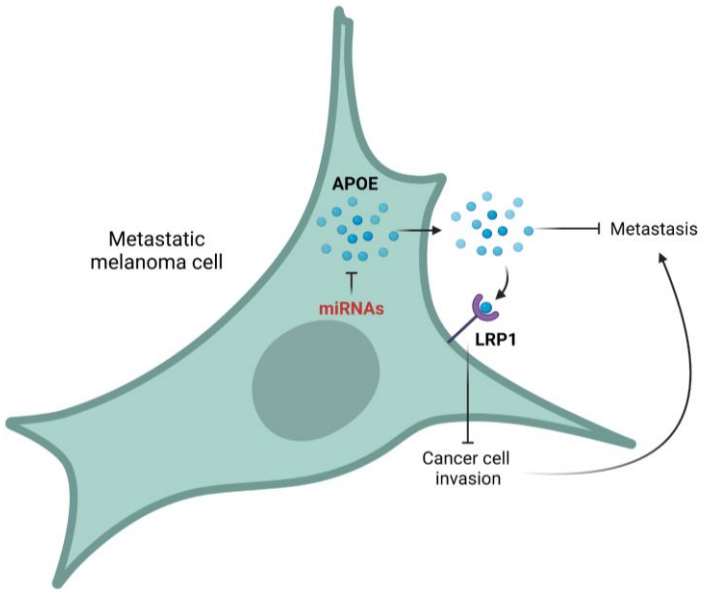

Figure 1.3 Schematic of the cell-autonomous role of APOE in melanoma. APOE secreted by melanoma cells binds to melanoma LRP1 receptors in an autocrine or paracrine manner. This leads to inhibition of invasiveness. Metastatic melanoma cells upregulate miRNAs that suppress their expression of APOE.

Similar to their disease impacts in the central nervous and cardiovascular systems, *APOE* genetic variants have now been shown to influence melanoma outcomes. Patients who carry an *APOE4* allele exhibit improved melanoma survival relative to *APOE3* homozygotes, whereas *APOE2* carriers experience the poorest outcomes (Ostendorf et al., 2020). This pattern was upheld in transplantable mouse models, in which subcutaneously injected melanoma tumors progressed faster in *APOE2* knock-in mice and slower in *APOE4* knock-in mice compared to *APOE3* mice. Through single-cell RNA-Seq, T cell depletion, and bone marrow transplantation experiments, it was determined that the *APOE4* genotype confers enhanced anti-tumor immunity. Consequently, *APOE4* mice and patients are more responsive to anti-PD1 immunotherapy. However, melanoma cells treated *in vitro*

with recombinant APOE variants in the absence of immune cells displayed an APOE4>APOE3>APOE2 pattern of suppression of invasion and endothelial cell recruitment. This implicates a poorly characterized cell-intrinsic impact of APOE variants on melanoma cell behavior. Importantly, these results showed how germline variation in a gene, in this case *APOE*, can modulate the progression of a future malignancy, as there was no difference in melanoma incidence between genotypes. This differs from most of our prior knowledge of how germline genetics impact cancer burden, where the predominant view has been that inherited polymorphisms mostly influence one's risk of developing cancer in the first place.

1.6 Overview

Apolipoprotein E has a substantial influence on human disease due to its genetic variation and diverse roles in mammalian physiology. This applies to melanoma as well. APOE has been shown to directly inhibit the metastatic capacity of melanoma cells, and allelic variation in the *APOE* gene influences melanoma survival. How *APOE* genetic variants differentially impact melanoma cell function and intracellular processes is unclear. The aim of this thesis was to determine cell-intrinsic effects of APOE variants on melanoma cells that could contribute to differences in melanoma progression among the *APOE* genotypes. Using a series of genetically engineered mouse models of melanoma expressing each of the three human APOE variants, I identify a biological axis between the APOE2 variant and its receptor LRP1 that enhances melanoma protein synthesis, growth, and metastasis. These findings

implicate a previously undescribed gain-of-function role of APOE2 in mRNA translation and highlight protein synthesis as a potential therapeutic vulnerability in melanoma.

CHAPTER 2. HUMAN *APOE* GERMLINE VARIANTS MODULATE GENETICALLY INITIATIED MELANOMA PROGRESSION

Previous studies in our laboratory investigating the role of APOE in melanoma progression have primarily utilized transplantable models, in which established cancer cells are injected directly into mice. A limitation of this approach is that it bypasses many steps of the metastatic cascade, and the APOE status of the cancer cell often does not match that of the mouse that is being injected. This chapter describes the generation and validation of a genetically engineered mouse model (GEMM) for melanoma that harbors each of the human APOE variants. We posited that because the melanomas formed in this model have the same genetics as the host and recapitulate every step of the metastatic process from tumor initiation through to metastatic colonization, all while in the presence of APOE, the differential impacts of APOE variants on melanoma cell function may be enriched.

2.1 Development of *APOE* allelic genetically engineered mouse model

To generate an *APOE* allelic GEMM, we utilized the well-established *Braf*$^{V600E/+}$*;Pten*$^{-/-}$*;Tyr::CreER* (BPC) mouse model. Using a tyrosinase promoter-driven Cre recombinase that is fused to the estrogen receptor, the BPC model enables inducible deletion of the *Pten* tumor suppressor and activation of the *Braf*^{V600E} oncogene specifically in melanocytes upon administration of 4-hydroxytamoxifen (4-OHT). This results in rapid melanoma formation in 3-4 weeks with 100% penetrance. The BPC model also recapitulates the entirety of the

metastatic cascade, as these mice can go on to form pigmented metastases in distant organs (Dankort *et al.*, 2009). We crossed this model with *APOE* knock-in mice in which the endogenous murine *Apoe* locus has been replaced with one of the three human *APOE* genes (Knouff *et al.*, 1999; Sullivan *et al.*, 1997; Sullivan *et al.*, 1998), thus generating BPC/APOE2, BPC/APOE3, and BPC/APOE4 mice **(Figure 2.1)**. As both tumor-derived and stromal APOE play roles in modulating the metastatic progression of melanoma (Pencheva et al., 2014; Pencheva et al., 2012), we predicted that allele-concordant host and tumoral APOE expression in this model would lead to substantial phenotypic effects.

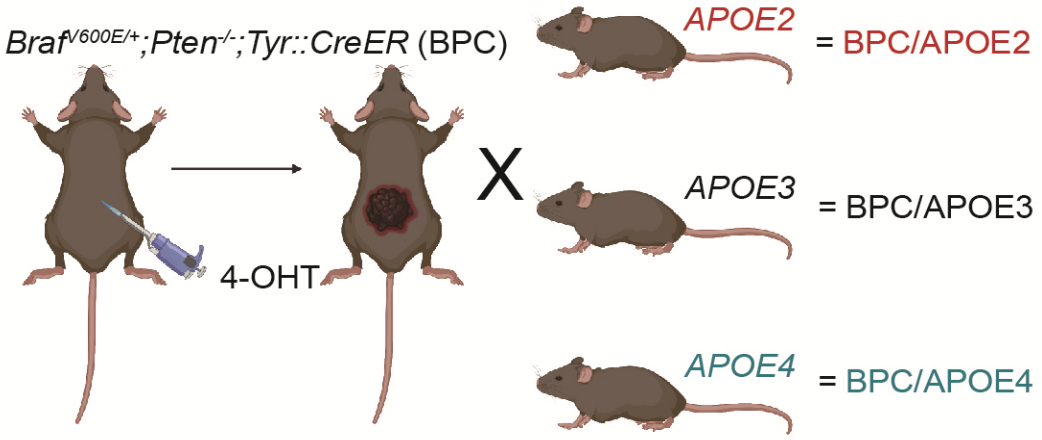

Figure 2.1. Generation of *APOE* allelic GEMM. Schematic depicting generation of and 4-hydroxytamoxifen (4-OHT) tumor induction in the *Braf* $^{V600E/+}$*;Pten* $^{-/-}$*;Tyr::CreER*;*APOE2* (BPC/APOE2), ;*APOE3* (BPC/APOE3), and ;*APOE4* (BPC/APOE4) mouse models.

2.2 APOE variants modulate primary tumor growth in genetically engineered mouse model

Having established an *APOE* allelic GEMM series, I next sought to validate whether this model recapitulated our previously described *APOE2>APOE3>APOE4* pattern of melanoma progression that was observed in transplantable mouse models and patient cohorts (Ostendorf *et al.*, 2020). After topical 4-OHT application to shaved back skin of adult mice, tumors (as defined by a visible, raised lesion) formed fastest in BPC/APOE2 mice, followed by BPC/APOE3 mice and BPC/APOE4 mice (**Figure 2.2**). This result suggests that the *APOE2* genetic background is most permissive to initial melanoma growth, while *APOE4* is the least permissive.

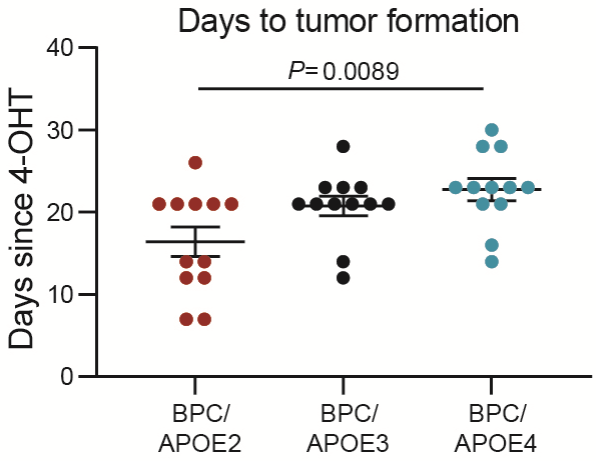

Figure 2.2 Days to tumor formation in *APOE* allelic GEMM. Number of days after topical 4-OHT administration until tumors were palpated and visualized in BPC/APOE2, BPC/APOE3, and BPC/APOE4 mice (n=12 per group). One-way ANOVA.

I next tracked survival of mice over time **(Figure 2.3a)**. Mice were euthanized when they reached a humane endpoint of marked tumor size, tumor ulceration,

weight loss, or lethargy. BPC/APOE2 mice had the shortest median survival at 42.5 days, BPC/APOE3 mice were intermediate at 53.5 days, and BPC/APOE4 mice had the longest survival at 59.5 days **(Figure 2.3b)**. These survival outcomes closely mirrored the survival outcomes observed in patient cohorts (Ostendorf *et al.*, 2020).

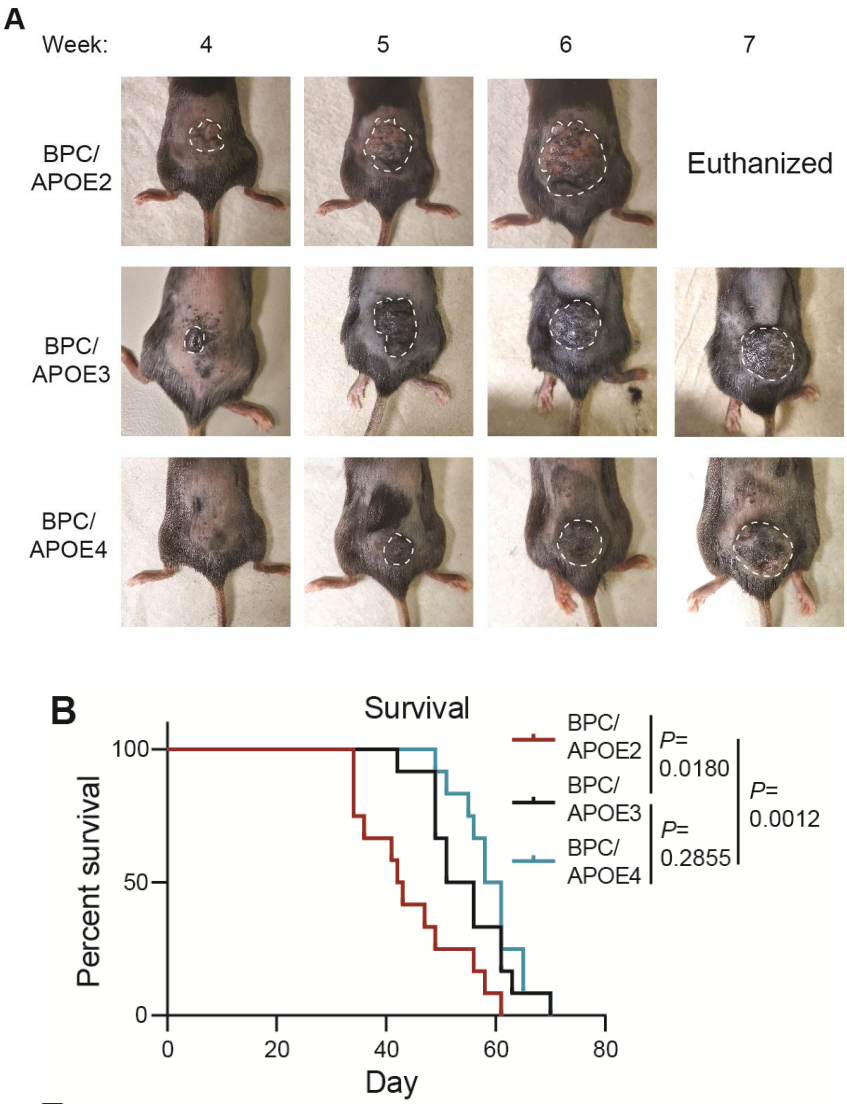

Figure 2.3 Survival outcomes in *APOE* allelic GEMM. (a) Representative images of tumor growth in BPC/APOE2, BPC/APOE3, and BPC/APOE4 mice 4 to 7 weeks after topical administration of 4-OHT. **(b)** Kaplan-Meier survival curves of BPC/APOE2, BPC/APOE3, and BPC/APOE4 mice after topical 4-OHT administration (n=12 per group). Log-rank test.

Having determined that BPC/APOE2 and BPC/APOE4 mice have the most divergent tumor progression phenotype, I focused mainly on the *APOE2* and *APOE4* genotypes for the remainder of this thesis. In an independent cohort of mice in which I tracked primary tumor growth rate, melanomas grew significantly faster **(Figure 2.4a)** and were significantly larger at the day 49 endpoint **(Figure 2.4b)** in BPC/APOE2 mice relative to BPC/APOE4 mice.

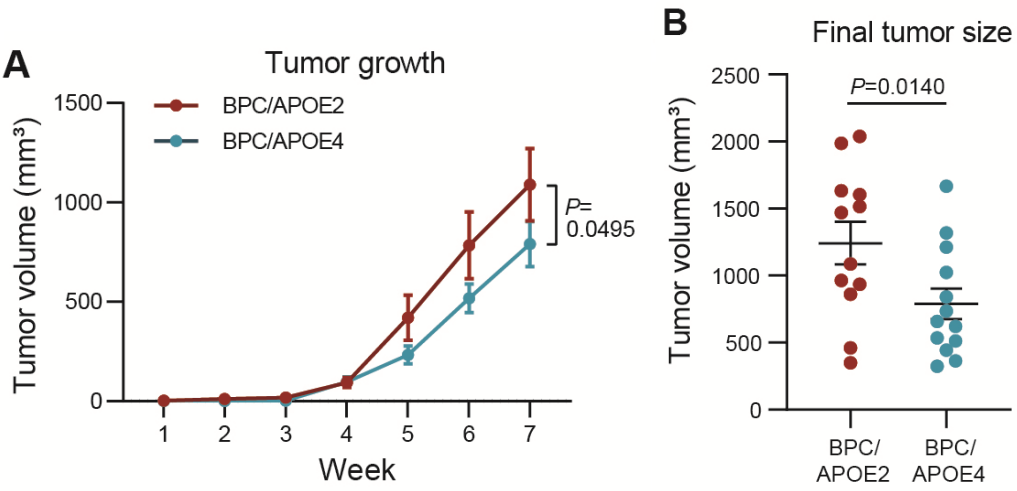

Figure 2.4 Primary tumor growth in *APOE* allelic GEMM. (a) Tumor growth curve of BPC/APOE2 (n=12) and BPC/APOE4 (n=13) mice after topical 4-OHT administration. Two-way ANOVA. **(b)** Final tumor volumes of BPC/APOE2 (n=12) and BPC/APOE4 (n=13) mice from **(a)** at the experimental endpoint of 49 days after topical 4-OHT administration. Unpaired t-test.

2.3 APOE variants differentially affect metastasis in genetically engineered mouse model

Despite thorough microscopic examination, I did not observe distant metastases in the adult mice utilized in the survival and primary tumor growth experiments described in Section 2.2. In fact, evaluation of metastatic burden in the BPC GEMM necessitates the topical administration of 4-OHT to newborn mice

within days of birth (Damsky et al., 2011). Accordingly, I administered 4-OHT to BPC/APOE2 and BPC/APOE4 neonates and euthanized them after weaning age to allow for the development of lung metastases. Pigmented foci were visible on the lung surface, and BPC/APOE2 mice exhibited substantially more lung metastatic burden compared to BPC/APOE4 mice **(Figure 2.5)**.

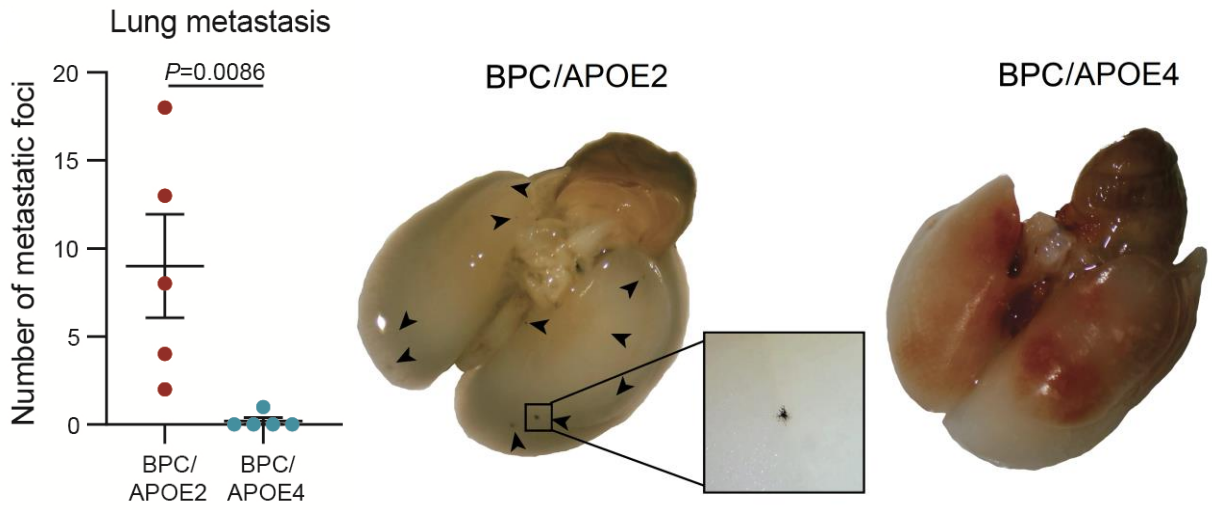

Figure 2.5 Metastatic progression in *APOE* allelic GEMM. Quantification of lung metastatic foci in BPC/APOE2 (n=5) and BPC/APOE4 (n=5) mice after neonatal tumor induction (left) and representative images of pigmented lung metastases from neonatal tumor induction in BPC/APOE2 mice (right). Arrows point to pigmented foci. Inset represents one metastatic focus at higher magnification. Unpaired t-test.

The differential impact of APOE variants on melanoma metastasis was more dramatic than that of primary tumor growth. The results in the APOE variant GEMM outlined in this chapter revealed a potent impact of hereditary genetics on primary tumor growth and metastatic dissemination in an autochthonous model of melanoma progression. Furthermore, they validated the model's utility as a tool for

investigating the effects of APOE variants on intrinsic melanoma cell molecular processes.

CHAPTER 3. IDENTIFCATION OF PROTEIN SYNTHESIS AS A CELL-INTRINSIC PATHWAY MODULATED BY APOE2

The molecular mechanisms underpinning APOE-mediated suppression of melanoma metastatic behavior are poorly characterized, and this applies even more so to the *APOE* genetic variants. This chapter describes the use of RNA-Seq in the *APOE* allelic GEMM described in Chapter 2 to identify intracellular processes that are differentially modulated between APOE variants. Through performing validation experiments, I make the surprising discovery that APOE2 activates protein synthesis in melanoma cells.

3.1 RNA-Seq reveals transcriptional upregulation of translation pathways in *APOE2* tumors relative to *APOE4*

Having established in Chapter 2 that the *APOE* allelic GEMM appropriately recapitulates the previously described *APOE2>APOE3>APOE4* severity of melanoma progression (Ostendorf *et al.*, 2020), I next utilized it as a tool to search for cellular processes that might be altered in an APOE variant-dependent manner and that could influence cancer progression. To this end, I performed bulk RNA-Seq of time-matched BPC/APOE2 and BPC/APOE4 tumors since they were the most phenotypically divergent. Gene set enrichment analysis (GSEA) (Subramanian et al., 2005) of gene expression revealed that translation was the most upregulated pathway in BPC/APOE2 tumors relative to BPC/APOE4 tumors **(Figure 3.1a)**. The additional protein synthesis-related pathways “Ribosomal RNA processing” and “Eukaryotic translation elongation” were also among the top ten upregulated

pathways. BPC/APOE2 tumors displayed significant upregulation in all major steps of translation present in the Reactome gene set (Jassal et al., 2019) relative to BPC/APOE4 tumors **(Figure 3.1b)**.

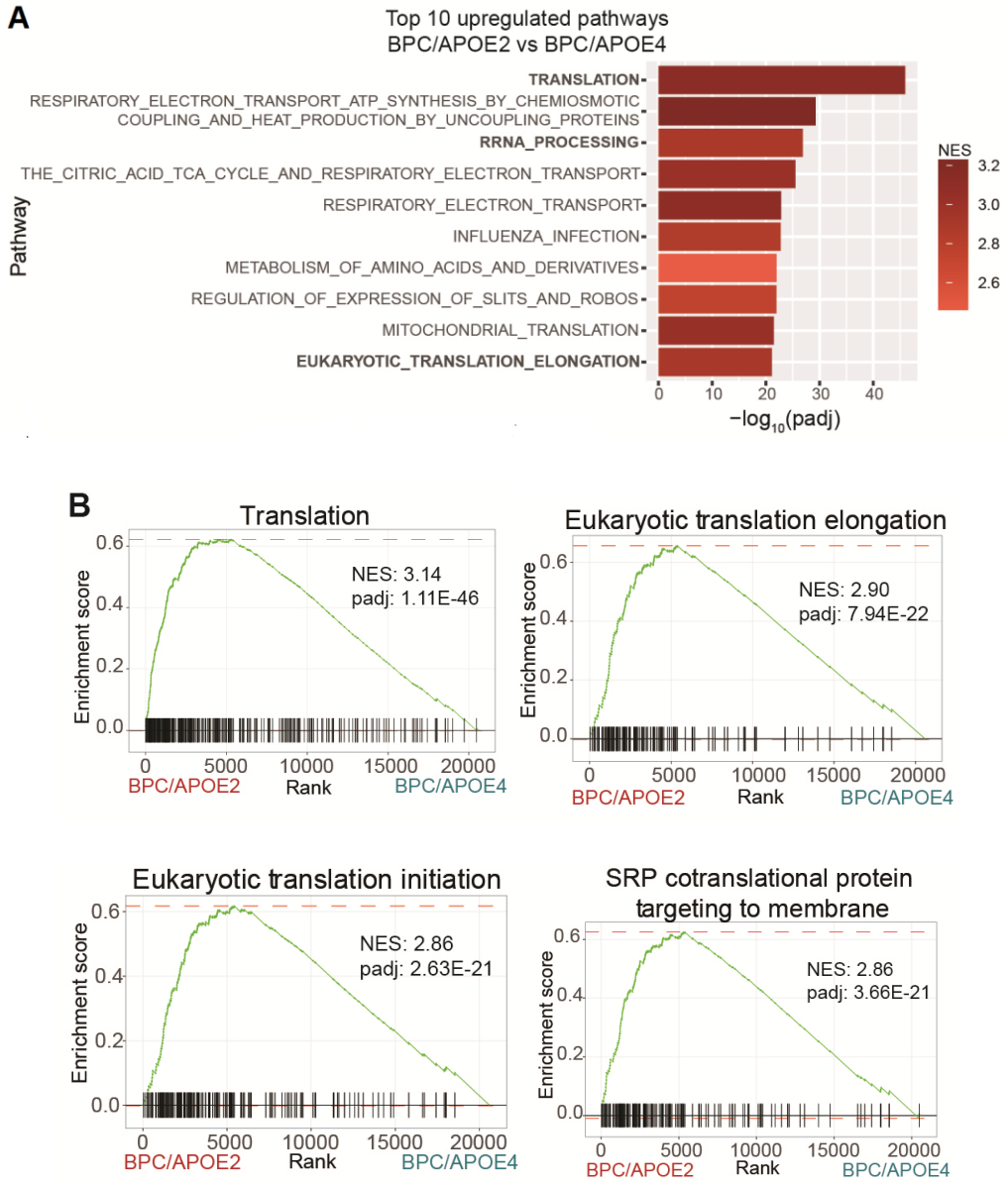

Figure 3.1 RNA-Seq pathways differentially regulated between BPC/APOE2 and BPC/APOE4 tumors. (a) Top ten pathways upregulated in melanomas of BPC/APOE2 mice relative to BPC/APOE4 mice as determined by GSEA and ranked by adjusted p-value (n=4 per group; NES, normalized enrichment score; padj, adjusted p-value). **(b)** Enrichment plots of translation-related pathways within the Reactome gene set.

3.2 *In vivo* validation of translational differences between *APOE2* and *APOE4* tumors

Translational control plays a crucial role in all steps of cancer progression from initiation through to metastatic dissemination, and most major oncogenic signaling pathways lead to the enhancement of tumor cell translational capacity (Truitt and Ruggero, 2016). Thus, translation appeared to be a promising pathway whose differential modulation by APOE variants could lead to significant changes in melanoma growth and metastasis. I therefore sought to experimentally validate whether there were differences in translational efficiency between *APOE2* and *APOE4* melanomas. I utilized the surface sensing of translation (SUnSET) assay, a well-established method for measuring protein synthesis (Schmidt et al., 2009). In this assay puromycin, a tyrosyl tRNA mimic, can be administered to live cells or mice, upon which it incorporates into nascent polypeptide chains (Goodman and Hornberger, 2013). Puromycin incorporation can then be quantified with an anti-puromycin antibody, providing a readout of global cellular translation **(Figure 3.2)**.

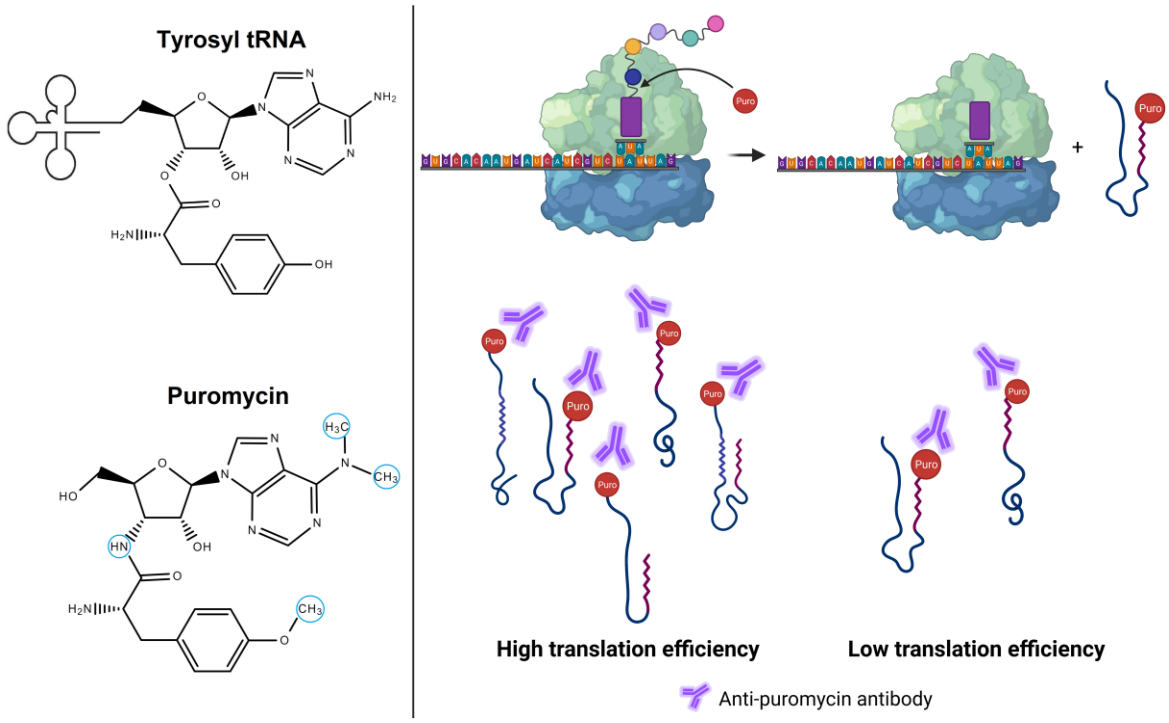

Figure 3.2 Principles of the SUnSET assay. The antibiotic puromycin is highly structurally similar to the tyrosyl tRNA. Differences between the molecules are highlighted in blue. In the presence of puromycin the ribosome transfers its actively synthesizing polypeptide chain from the bound tyrosyl tRNA to a puromycin molecule, causing dissociation of the nascent peptide. Puromycylated peptides can then be detected with an anti-puromycin antibody. Cells with highly active translation machinery will produce more puromycylated peptides, thus leading to stronger antibody signal.

To control for tumor size differences, I intraperitoneally injected BPC/APOE2 and BPC/APOE4 mice with puromycin 35 days after 4-OHT administration, an early time point at which a significant difference in tumor volumes was not yet detectable **(Figure 3.3)**. Consistent with the RNA-Seq results detailed in section 3.1, BPC/APOE2 tumors exhibited significantly higher puromycin incorporation than BPC/APOE4 tumors, indicative of either a slower translation rate in the *APOE4* background or enhanced translation rate in the *APOE2* background **(Figure 3.4)**.

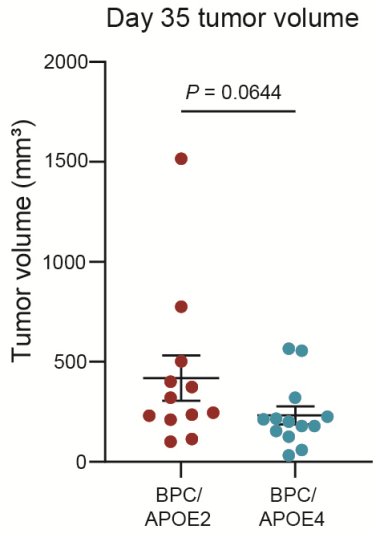

Figure 3.3 Early tumor size comparison of BPC/APOE2 and BPC/APOE4 mice. Tumor volumes of BPC/APOE2 (n=12) and BPC/APOE4 (n=13) mice 35 days after 4-OHT administration. Unpaired t-test.

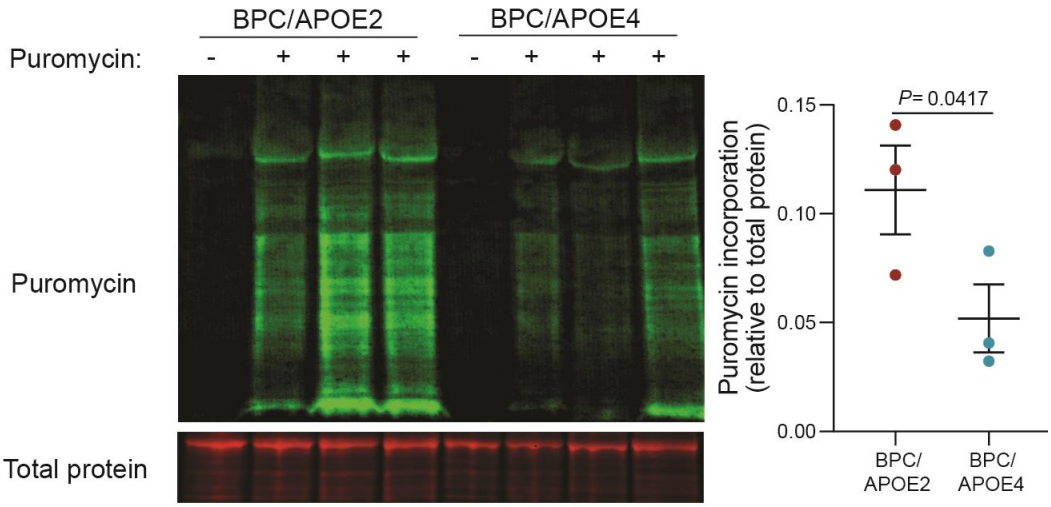

Figure 3.4 *In vivo* SUnSET assay. Western blot of puromycin incorporation into BPC/APOE2 and BPC/APOE4 tumors 35 days after 4-OHT administration (n=3 per group). Non-puromycin-pulsed mice were included as an antibody control. Unpaired t-test.

3.3 *In vitro* validation of effects of APOE variants on protein synthesis and identification of gain-of-function activity of APOE2

Despite the use of size-matched tumors, *in vivo* puromycin incorporation can be confounded by differences in proliferation rate or uptake by non-tumor cells in the microenvironment such as fibroblasts. To control for these confounders, I performed the SUnSET assay *in vitro* using mouse APOE-depleted B16F10 murine melanoma cells stably overexpressing APOE2, APOE3, APOE4, or an empty control vector **(Figure 3.5)**. Strikingly, there was no difference in puromycin incorporation between control, APOE3, and APOE4 cells, whereas APOE2-expressing cells exhibited substantially increased puromycin signal **(Figure 3.6)**.

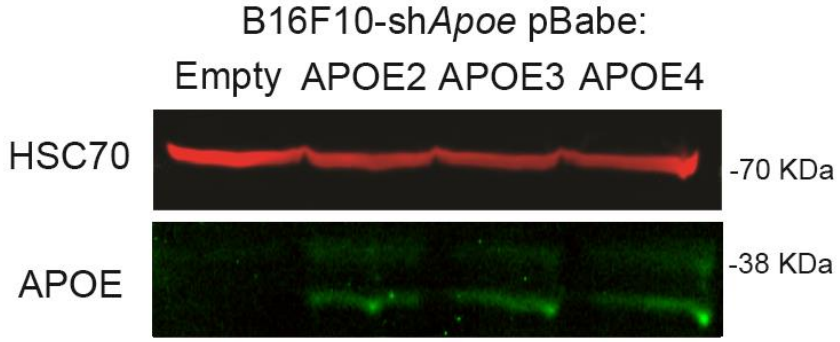

Figure 3.5 Stable overexpression of APOE variants. Western blot of APOE expression in B16F10-sh*Apoe* cells transduced with pBabe Empty, APOE2, APOE3, or APOE4 retrovirus. HSC70 served as a loading control.

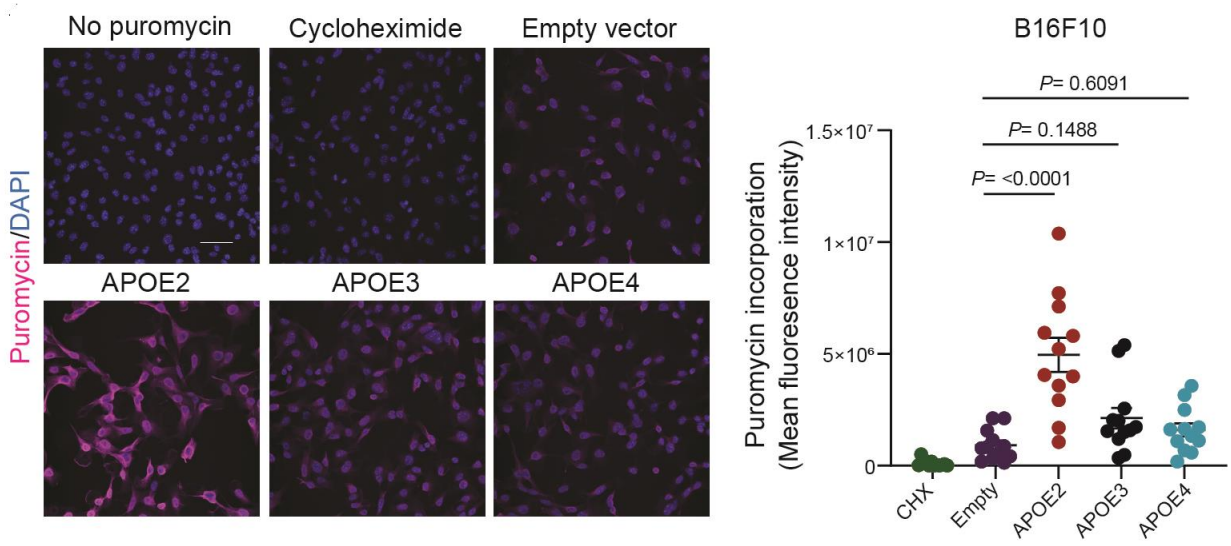

Figure 3.6 *In vitro* SUnSET assay. Representative immunofluorescence images (left) and quantification of mean fluorescence intensity (right) of puromycin incorporation into B16F10-sh*Apoe* pBabe Empty, APOE3, APOE2, and APOE4 cells. Non-puromycin-pulsed and cycloheximide (CHX)-treated cells were included as negative and positive controls, respectively (scale bar = 50μM). One-way ANOVA (n=3 independent experiments).

These results are consistent with a model whereby APOE2 promotes translation rather than APOE4 inhibiting translation. To our knowledge, this is a previously uncharacterized gain-of-function role of APOE2 in which it acts to enhance cellular protein synthesis. Thus, rather than simply being defective at promoting anti-tumor immunity (Ostendorf *et al.*, 2020), APOE2 may actively promote more aggressive melanoma progression by activating tumoral protein synthesis.

CHAPTER 4. ROLE OF TUMORAL APOE RECEPTOR EXPRESSION

The effects of APOE2 on melanoma protein synthesis described in Section 3 established a direct impact of APOE on a melanoma intracellular process. Our lab previously reported that the APOE receptor LRP1, expressed by the melanoma cells, mediates the cell-autonomous effects of APOE on invasion and metastasis (Pencheva *et al.*, 2012). Thus, we hypothesized that LRP1 may be involved in the gain-of-function activity of APOE2 and ultimately the differential modulation of melanoma progression by APOE variants. This chapter explores the consequences of tumoral LRP1 loss on melanoma progression and protein synthesis in the context of APOE variants.

4.1 Tumoral *Lrp1* deletion abrogates APOE variant differences in tail vein metastatic capacity

We previously observed that murine APOE-depleted B16F10 mouse melanoma cells metastasize to the lung more efficiently in *APOE2* knock-in mice compared to *APOE4* mice after injection via the lateral tail vein (Ostendorf *et al.*, 2020). Therefore, to determine whether LRP1 mediates the effects of APOE variants on metastatic capacity, I performed CRISPR/Cas9-mediated deletion of LRP1 in B16F10-sh*Apoe* cells **(Figure 4.1)**.

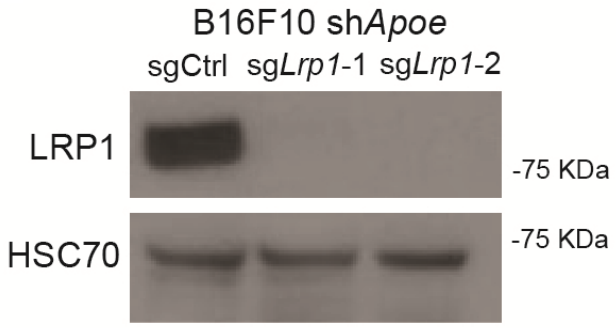

Figure 4.1 CRISPR-mediated deletion of LRP1 in melanoma cells. Western blot of LRP1 expression in B16F10-TR-sh*Apoe* cells transfected with a non-targeting control CRISPR sgRNA or two independent *Lrp1*-targeting sgRNAs. HSC70 served as a loading control.

Melanoma cells transduced with a non-targeting control guide RNA (sgRNA) metastasized to the lung more efficiently in *APOE2* knock-in mice compared to *APOE4* knock-in mice after tail vein injection, thus validating our previous observations **(Figure 4.2a)**. However, upon *Lrp1* deletion with two independent sgRNAs, the difference in metastatic burden between *APOE2* and *APOE4* mice was abolished **(Figure 4.2b)**. This finding reveals that the effects of APOE variants on melanoma metastatic capacity are mediated by the APOE receptor LRP1.

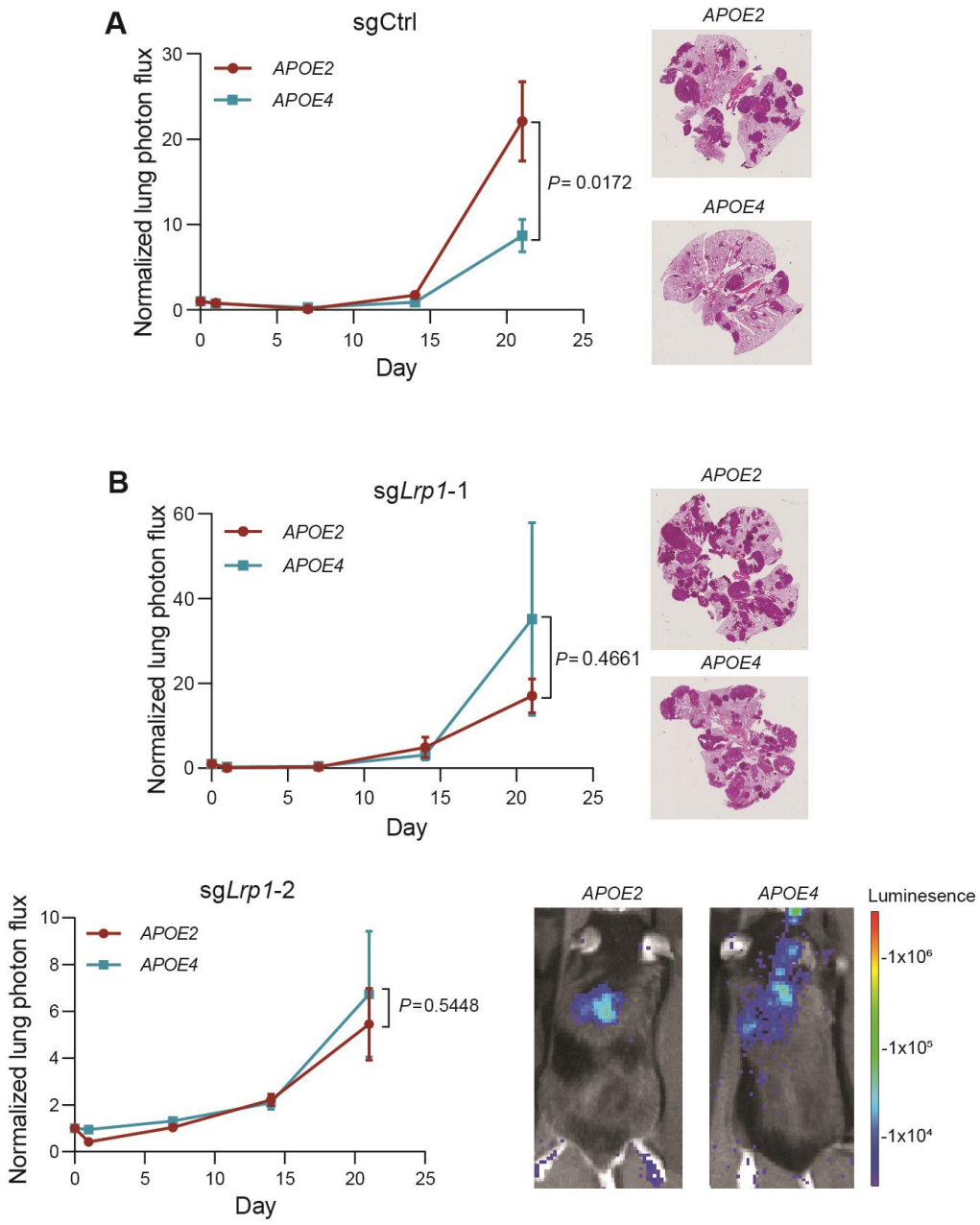

Figure 4.2 LRP1 mediates effects of APOE variants on tail vein metastasis. Quantification of lung metastatic progression via bioluminescence imaging of B16F10-TR-sh*Apoe* sgCtrl **(A)** or sg*Lrp1* **(B)** cells injected via lateral tail vein into *APOE2* and *APOE4* mice. Representative images of H&E-stained lungs or bioluminescence signal taken from mice at the day 21 endpoint (n= 9-10 mice per group; representative of two independent experiments; two-way ANOVA).

4.2 Tumoral *Lrp1* deletion abrogates APOE variant differences in genetically initiated melanoma progression

As discussed in Chapter 2, a major limitation of transplantable mouse models such as the tail vein metastasis assay is that many steps of the metastatic cascade are bypassed. Furthermore, the melanoma cells used in Section 4.1 do not express human *APOE* in concordance with their knock-in mouse host. To overcome these limitations and better interrogate the role of LRP1 in APOE variant modulation of melanoma progression, I crossed the BPC/APOE2 and BPC/APOE4 GEMMs with *Lrp1*$^{flox/flox}$ mice. This enables deletion of *Lrp1* specifically in the melanocytes that will go on to form melanomas after 4-OHT administration. Immunofluorescence staining of BPC/APOE2*;Lrp1*$^{flox/flox}$ (BPC/APOE2/LRP1Δ) and BPC/APOE4*;Lrp1*$^{flox/flox}$ (BPC/APOE4/LRP1Δ) tumors showed substantial loss of LRP1 signal compared to *Lrp1* wild-type tumors, confirming successful Cre-mediated deletion **(Figure 4.3)**.

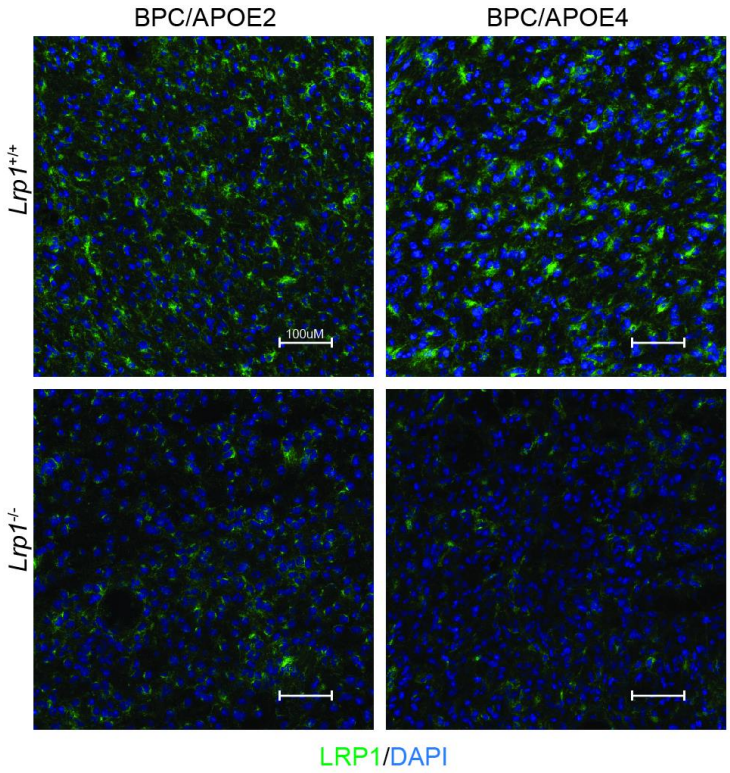

Figure 4.3 Validation of Cre-mediated *Lrp1* deletion in GEMM. Representative immunofluorescence images of LRP1 expression and DAPI nuclear staining in BPC/APOE2, BPC/APOE4, BPC/APOE2/LRP1Δ, and BPC/APOE4/LRP1Δ primary tumors (scale bar = 100 μm).

Similar to the analyses performed in Chapter 2, I monitored tumor growth in BPC/APOE2/LRP1Δ and BPC/APOE4/LRP1Δ mice after 4-OHT administration to back skin. In contrast to the differential effects of APOE variants observed in *Lrp1* wild-type mice, there was no significant difference in tumor latency **(Figure 4.4a)**, tumor growth rate **(Figure 4.4b)**, or tumor volume at the experimental endpoint **(Figure 4.4c)** between BPC/APOE2/LRP1Δ and BPC/APOE4/LRP1Δ mice. In a separate survival experiment, there was a significant difference with BPC/APOE2/LRP1Δ mice having a median survival of 55 days compared to 63 days in BPC/APOE4/LRP1Δ mice **(Figure 4.4d)**. However, this difference was highly

diminished compared to *Lrp1* wild-type BPC/APOE2 and BPC/APOE4 mice **(Figure 2.3b)**. This result is consistent with our prior findings revealing that the *APOE4* background confers more potent anti-tumor immunity and repressed angiogenesis (Ostendorf *et al.*, 2020), thus likely providing BPC/APOE4/LRP1Δ mice a survival advantage over BPC/APOE2/LRP1Δ mice at later primary tumor stages. There was no significant difference in distant lung metastasis between BPC/APOE2/LRP1Δ and BPC/APOE4/LRP1Δ mice after neonatal 4-OHT administration **(Figure 4.4e)**, consistent with LRP1-dependent, cell-intrinsic effects of APOE dominating at the metastatic site. These results indicate that *Lrp1* deletion significantly abrogates the impact of APOE variants on melanoma progression, with differences only emerging when the cell-extrinsic effects of APOE dominate at later primary tumor stages in the genetic model.

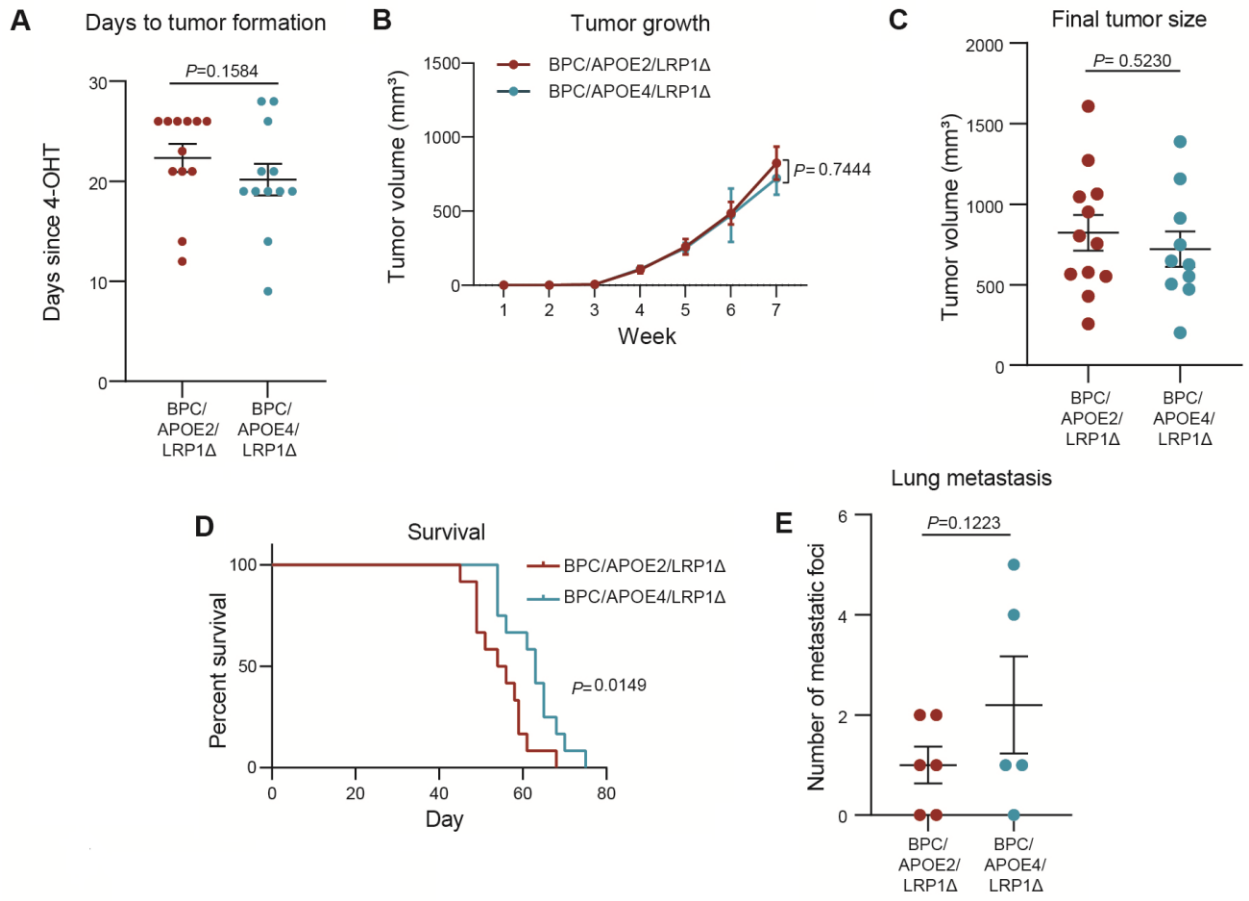

Figure 4.4 Melanocyte-specific *Lrp1* deletion abrogates differences in melanoma progression between *APOE2* and *APOE4* GEMMs. (A) Number of days after topical 4-OHT administration until tumors were palpated and visualized in BPC/APOE2/LRP1Δ and BPC/APOE4/LRP1Δ mice (n=12 per group). Unpaired t-test. **(B)** Melanoma tumor growth curves of BPC/APOE2/LRP1Δ (n=12) and BPC/APOE4/LRP1Δ (n=10) mice after topical 4-OHT administration. Two-way ANOVA. **(C)** Final tumor volumes of BPC/APOE2/LRP1Δ (n=12) and BPC/APOE4/LRP1Δ (n=10) mice at the experimental endpoint 49 days after topical 4-OHT administration. Unpaired t-test. **(D)** Kaplan-Meier survival curves of BPC/APOE2/LRP1Δ and BPC/APOE4/LRP1Δ mice after topical 4-OHT administration (n=12 per group). Log-rank test. **(E)** Quantification of lung metastatic foci in BPC/APOE2/LRP1Δ (n=6) and BPC/APOE4/LRP1Δ (n=5) mice after neonatal tumor induction. Unpaired t-test.

Of note, equalization of melanoma progression between BPC/APOE2 and BPC/APOE4 mice upon LRP1 deletion was largely driven by diminished tumor growth and metastasis in the *APOE2* background. This can be best visualized by aggregating data from Chapter 2. Tumor progression and metastasis between BPC/APOE4 and BPC/APOE4/ LRP1Δ mice was unchanged while BPC/APOE2/ LRP1Δ melanomas were less aggressive than BPC/APOE2 melanomas **(Figure 4.5)**. These results again support the model that APOE2 is acting in a gain-of-function manner to promote melanoma progression, and that this is dependent on tumoral LRP1 expression.

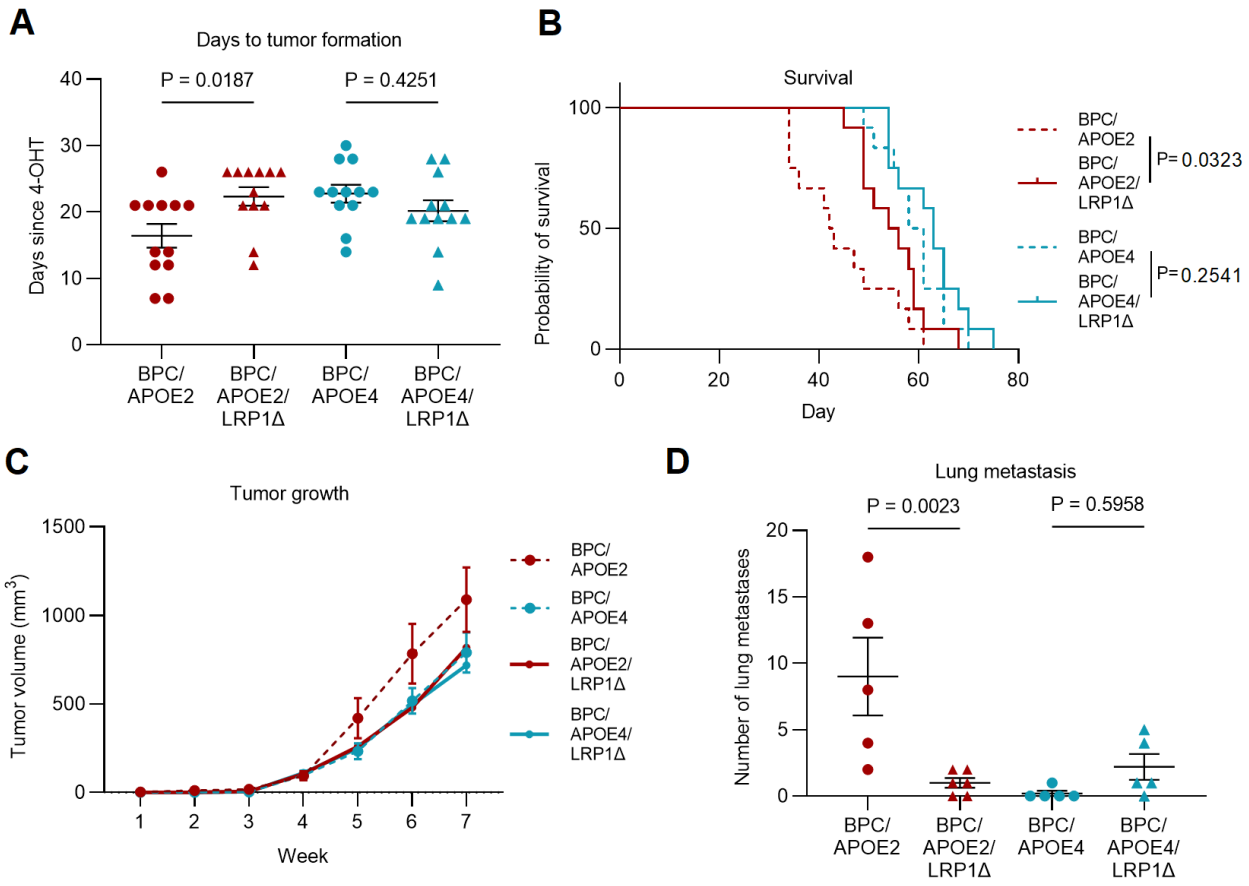

Figure 4.5 Comparison of progression in LRP1 wild-type and knockout BPC mice highlights melanoma-promoting effect of APOE2. (A) Comparison of number of days after topical 4-OHT administration until visible, palpable tumors formed in BPCE/APOE2, BPC/APOE2/LRP1Δ, BPC/APOE4, and BPC/APOE4/ LRP1Δ mice (n=12 per group). One-way ANOVA. **(B)** Comparison of Kaplan-Meier survival curves of BPCE/APOE2, BPC/APOE2/LRP1Δ, BPC/APOE4, and BPC/APOE4/ LRP1Δ mice after topical 4-OHT administration (n=12 per group). Log-rank test. **(C)** Comparison of tumor growth curves of BPCE/APOE2 (n=12), BPC/APOE2/LRP1Δ (n=12), BPC/APOE4 (n=13), and BPC/APOE4/ LRP1Δ (n=10) mice after topical 4-OHT administration. **(D)** Comparison of lung metastatic foci in BPCE/APOE2 (n=5), BPC/APOE2/LRP1Δ (n=6), BPC/APOE4, and BPC/APOE4/ LRP1Δ (n=5) mice after neonatal tumor induction. One-way ANOVA.

4.3 Tumoral *Lrp1* deletion abrogates APOE variant differences in protein synthesis

Having determined that LRP1 mediates the cell-intrinsic effects of APOE variants on melanoma progression, I next investigated whether APOE2-mediated enhancement of melanoma protein synthesis (Chapter 3) is LRP1-dependent. This would link the impact of APOE2 on this intracellular process with the more aggressive tumor growth and metastasis phenotypes that I observe in *APOE2* mice. I performed the SUnSET assay with time-matched BPC/APOE2/LRP1Δ and BPC/APOE4/LRP1Δ tumors. Results revealed equalization of puromycin incorporation between the *APOE2* and *APOE4* genotypes upon *Lrp1* deletion. This establishes an APOE2-LRP1 axis in melanoma that enhances pro-tumorigenic protein synthesis **(Figure 4.6)**.

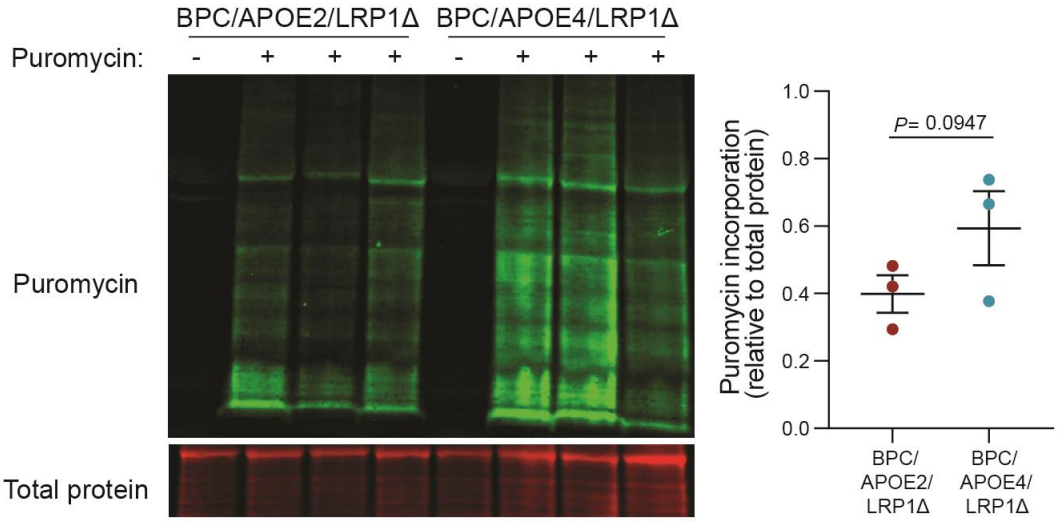

Figure 4.6 *In vivo* SUnSET assay in LRP1-deficient *APOE* allelic GEMM. Western blot of puromycin incorporation into BPC/APOE2/LRP1Δ and BPC/APOE4/LRP1Δ tumors 35 days after topical 4-OHT administration (n=3 per group). Non-puromycin-pulsed mice were included as an antibody control. Unpaired t-test.

The findings outlined in this chapter reveal that the APOE receptor LRP1 is a required mediator of the effects of APOE variants on melanoma progression at the early primary tumor and metastasis stages. Moreover, LRP1 is required for the enhanced protein synthesis effect mediated by APOE2 in melanoma tumors. Linking these observations together, it is likely that the more aggressive nature of *APOE2* melanomas is partly driven by APOE2 acting in a gain-of-function manner to promote translation in melanoma cells, thus providing them an advantage in growth and metastasis.

CHAPTER 5. CELL-INTRINSIC PATHWAY MODULATION BY APOE VARIANTS IN HUMAN MELANOMA

The *APOE* allelic GEMM closely mirrored the *APOE2*<*APOE3*<*APOE4* order of human melanoma survival outcomes that our lab previously reported (Ostendorf *et al.*, 2020). As a result, it served as a powerful tool to identify protein synthesis as a melanoma cell-intrinsic process that is activated by APOE2. I next wanted to determine whether this mechanism translated to human melanomas. To this end, I leveraged The Cancer Genome Atlas skin cutaneous melanoma (TCGA-SKCM) cohort, which contains over 400 patients with both RNA sequencing and whole exome sequencing data (Cancer Genome Atlas Network, 2015). I paired the *APOE* genotype status of each patient, previously imputed by my colleague Benjamin Ostendorf based on their whole exomes, with their tumor transcriptome. I then performed differential gene expression analysis of *APOE2* versus *APOE4* carrier tumors, analyzing primary and metastatic tumors separately **(Figure 5.1)**.

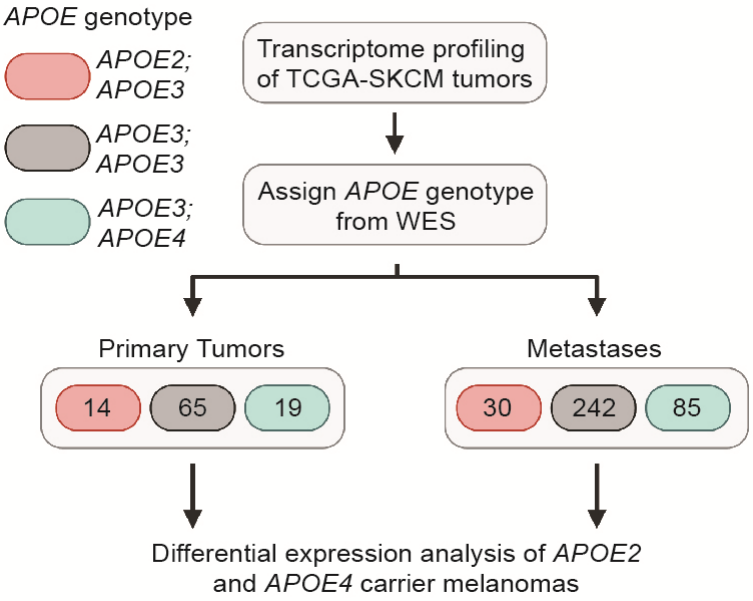

Figure 5.1 TCGA analysis workflow. Schematic depicting the workflow utilized to analyze transcriptomes of melanomas in the TCGA-SKCM cohort based on patient's *APOE* genotype (WES, whole exome sequencing).

Consistent with my RNA-Seq analysis in BPC/APOE2 and BPC/APOE4 mice, primary tumors from *APOE2* carrier patients exhibited significantly upregulated translation pathways relative to *APOE4* carriers **(Figure 5.2a)**. By performing the SUnSET assay in BPC/APOE2 and BPC/APOE4 mice, I established experimentally in Chapter 3 that upregulation of translation processes at the transcriptomic level correlates well with enhanced protein synthesis capacity. Thus, this result suggests that melanomas in patients who carry an *APOE2* allele are synthesizing proteins more efficiently than melanomas in *APOE4* carrier patients. Supporting the notion that APOE2 is an active promoter of protein synthesis in both mouse and human melanoma, translation pathways were also the top upregulated processes in *APOE2* carrier primary tumors compared to *APOE3* homozygotes **(Figure 5.2b)**. In contrast,

protein synthesis processes were not among the top upregulated pathways in *APOE3* tumors compared to *APOE4*, suggesting that mRNA translation is not a primary mediator of the survival difference between *APOE3* homozygotes and *APOE4* carrier patients **(Figure 5.2c)**.

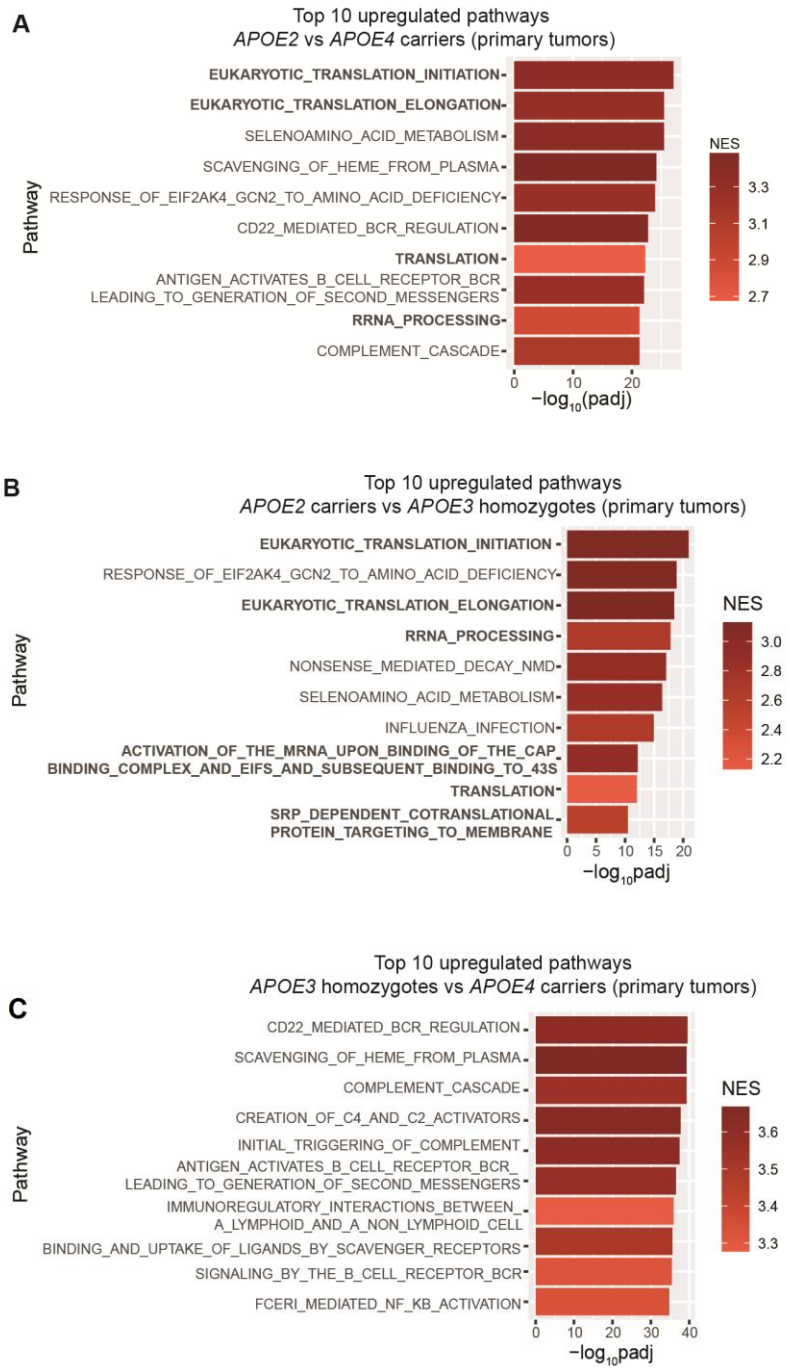

Figure 5.2 *APOE2* carrier patient primary melanomas exhibit translation upregulation. (A) Top ten pathways upregulated in primary tumors of *APOE2* carrier patients (n=14) relative to *APOE4* carrier patients (n=19) as determined by GSEA and ranked by adjusted p-value (NES, normalized enrichment score; padj, adjusted p-value). **(B)** Top ten pathways upregulated in primary tumors of *APOE2* carrier patients (n=14) relative to *APOE3* homozygotes (n=65). **(C)** Top ten pathways upregulated in primary tumors of *APOE3* homozygotes (n=65) relative to *APOE4* carrier patients (n=19).

Translation upregulation in the *APOE2* background relative to *APOE4* was also maintained in metastatic tumors, suggesting that APOE2 promotes protein synthesis in the melanomas of *APOE2* carriers throughout the metastatic cascade **(Figure 5.3)**.

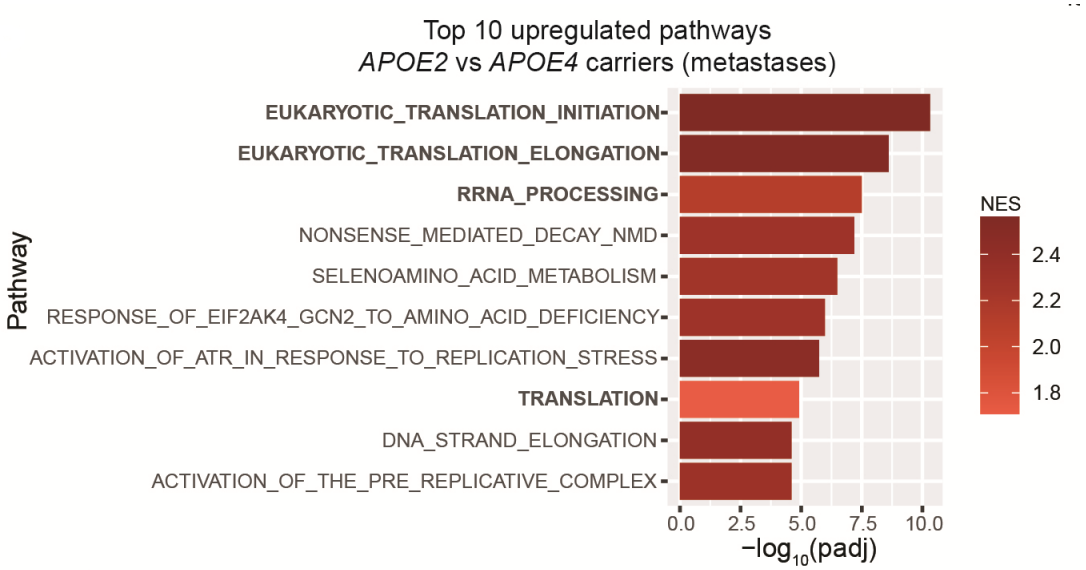

Figure 5.3 *APOE2* carrier metastatic melanomas exhibit translation upregulation. Top ten pathways upregulated in metastases of *APOE2* carrier patients (n=30) relative to *APOE4* carrier patients (n=85) as determined by GSEA and ranked by adjusted p-value.

Taken together with my findings from mouse modeling, we propose that APOE2-mediated enhancement of translation – a key driver of tumor growth and metastasis – supports melanoma progression in *APOE2* carriers, consistent with their poor survival compared to both *APOE3* homozygotes and *APOE4* carriers.

CHAPTER 6. DISCUSSION

6.1 Major findings

In this thesis I sought to identify melanoma cell-intrinsic processes that are differentially modulated by *APOE* genetic variants that may contribute to their disparate effects on melanoma progression. To this end, we crossed a genetically engineered mouse model (GEMM) characterized by melanocyte-specific activation of the *BRAF V600E* oncogene and loss of the *PTEN* tumor suppressor with mice bearing each of the three human *APOE* variants. This model enables concordant *APOE* variant expression between both the tumoral and stromal compartments, as it occurs in patients. Consistent with previous findings in transplantable models as well as patient cohorts (Ostendorf *et al.*, 2020), primary tumor growth in this genetic model progressed fastest in *APOE2* mice and slowest in *APOE4* mice, with *APOE3* tumor growth intermediate. Unlike transplantable models, GEMMs recapitulate each step of the metastatic cascade from tumor initiation through to distant colonization. Furthermore, both tumoral and stromal APOE contribute to modulation of melanoma metastasis (Pencheva *et al.*, 2014). I observed a potent effect of APOE variants on metastatic capacity in the genetic model, whereby lung metastatic burden was dramatically higher in *APOE2* mice compared to *APOE4* mice. I thus show a powerful effect of germline genetic variation in the *APOE* gene on growth and metastasis of *de novo* melanoma.

To identify cellular processes that are regulated in an APOE variant-dependent manner, I performed bulk RNA-seq of primary tumors derived from the *APOE2* and *APOE4* GEMMs. Gene set enrichment analysis revealed mRNA translation as the most impacted pathway, with significant upregulation in *APOE2* mice relative to *APOE4* mice. To experimentally validate these findings, I performed puromycin incorporation assays to determine differences in translational efficiency among the APOE variants. After peritoneal puromycin injection, tumors from the *APOE2* GEMM exhibited significantly higher puromycin incorporation than *APOE4* mice, confirming enhanced protein synthesis in the *APOE2* background. I repeated this assay *in vitro* with melanoma cells stably expressing each of the human APOE variants to control for differences in proliferation and the contribution of stromal cells; this revealed that APOE2 expression actively enhanced protein synthesis. Thus, APOE2 enhances protein synthesis in melanoma, likely contributing to the more aggressive progression of melanoma in the *APOE2* genetic background. These results are the first identification of APOE2 acting in a gain-of-function manner as an activator of protein synthesis, to our knowledge.

Due to previous work in our lab showing that the LRP1 receptor mediates the cell-autonomous effects of APOE on melanoma metastasis (Pencheva *et al.*, 2012), I sought to determine whether the differential effects of APOE variants on melanoma progression are dependent on LRP1. Murine melanoma cells injected via tail vein metastasized to the lung significantly more efficiently in *APOE2* mice compared to *APOE4* mice, but this difference was abrogated in melanoma cells depleted of LRP1

expression. After integrating conditional *Lrp1* deletion into the BPC GEMM, I observed that differences in primary tumor growth, metastasis, and protein synthesis rates between *APOE2* and *APOE4* mice were nullified as LRP1-deficient APOE2 tumors became less aggressive than LRP1 proficient APOE2 tumors. These results provide genetic support for an APOE2/LRP1 axis that promotes melanoma progression.

I next sought to determine whether APOE2 also enhances protein synthesis in patient tumors, thus potentially contributing to the poor melanoma survival outcomes of *APOE2* carriers. I analyzed RNA-seq data of primary and metastatic melanomas in the TCGA-SKCM study using *APOE* genotype status previously determined by analysis of whole exome sequencing data (Cancer Genome Atlas Network, 2015; Ostendorf *et al.*, 2020). Consistent with my mouse findings, translation pathways were the most significantly upregulated in both the primary and metastatic tumors of *APOE2* carriers compared to *APOE4* carriers. This upregulation was observed when comparing tumors of *APOE2* carriers and *APOE3* homozygotes as well. These findings suggest that the confluence of enhanced tumor protein synthesis along with poor anti-tumor immunity, invasion inhibition, and angiogenesis repression in *APOE2* carriers contributes to their dramatically impaired prognosis **(Figure 6)**.

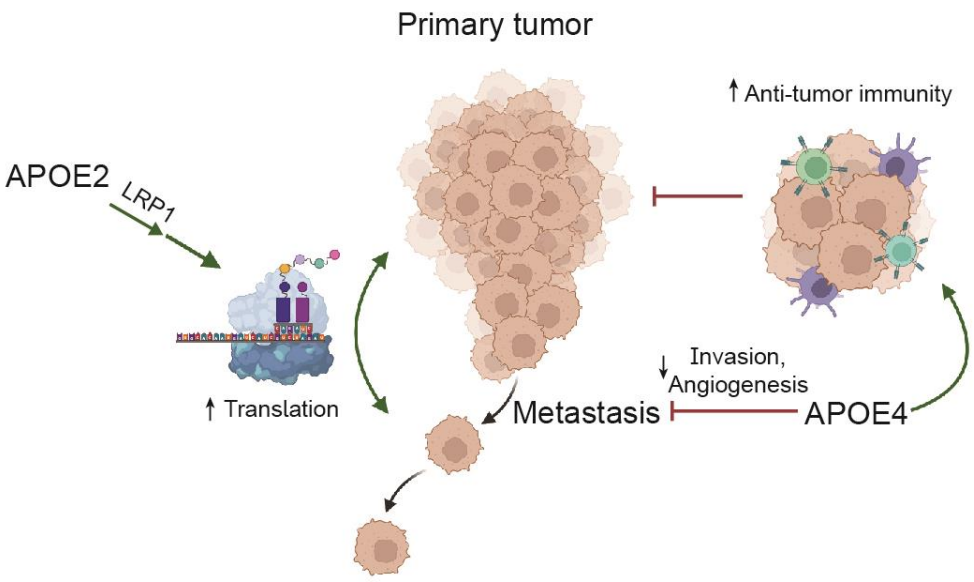

Figure 6. Opposing roles of APOE2 and APOE4 in melanoma progression. Model depicting our current understanding of the role of APOE2 and APOE4 in melanoma progression. The model depicts APOE4 acting as a suppressor of melanoma growth and metastasis by enhancing anti-tumor immunity as well as repressing angiogenesis and invasion. In contrast, APOE2 is shown as a driver of melanoma progression through its stimulation of protein synthesis via the LRP1 receptor.

6.2 Clinical relevance

Despite a wave of recent advances in melanoma treatment, the 5-year survival of individuals with metastatic disease remains at only approximately 30% (Surveillance Research Program, 2022). There remains a great need to identify patients at greatest risk of metastatic progression as well as additional therapeutic vulnerabilities that can be exploited for new treatments. The findings outlined in this thesis provide further evidence that *APOE* genotype may serve as a potential biomarker for identifying those most at risk for metastatic progression. In addition to suboptimal anti-tumor immunity that enables enhanced primary tumor growth and poor response to immunotherapy (Ostendorf et al., 2020), I observed that

melanomas in *APOE2* carrier patients exhibit more efficient protein synthesis. Thus, *APOE2* carriers may be identified as individuals who need more aggressive therapy and closer monitoring. Future clinical studies, such as prospective trials, will be needed to determine whether *APOE* genotype status may serve as a clinically meaningful prognostic indicator.

The current mainstays of melanoma pharmaceutical intervention are MAPK pathway-targeted therapies and immune checkpoint inhibitors. However approximately 50% of melanomas are *BRAF* wild-type, and there is an absence of targeted therapies available for these individuals. Additionally, up to 42% of melanoma patients are completely resistant to immune checkpoint blockade, and many initial responders to anti-CTLA-4 and anti-PD-1 therapies will acquire resistance over time (Larkin et al., 2019). My results suggest that targeting protein synthesis may be a beneficial therapeutic strategy in melanoma, as more aggressive *APOE2* melanomas are characterized by enhanced translational capacity. Though many inhibitors are currently in clinical trials, the only prominent protein synthesis inhibitors that have had consistent clinical use in cancer treatment are derivatives of the mTOR inhibitor rapamycin. Temsirolimus was approved by the FDA for the treatment of advanced renal carcinoma in 2007. Everolimus was first FDA-approved in 2009 for the treatment of advanced renal cell carcinoma, and its use has since been expanded to neuroendocrine tumors, breast cancer, and the prevention of transplant rejection (Conciatori et al., 2018). Rapamycin has been shown to be effective against tumor growth in the BPC GEMM (Dankort *et al.*, 2009).

Furthermore, resistance to BRAF and MEK combination therapy involves the activation of mTOR signaling, thus making targeted therapy-resistant melanoma susceptible to mTOR inhibition (Wang et al., 2021). Combined MEK and PI3K/mTOR inhibition has also shown experimental efficacy in NRAS-mutant melanoma, for which there are currently no targeted therapies (Posch et al., 2013). More recently another translation inhibitor named omacetaxine, formerly known as homoharringtone, was approved for the treatment of refractory chronic myelogenous leukemia in 2012. This drug inhibits translation elongation by binding to ribosomes, thus making it the first clinically approved direct inhibitor of mRNA translation (Gandhi et al., 2014). Future experimental studies of these inhibitors' effects in melanoma in the context of APOE2 expression are warranted. This could involve monitoring tumor progression in BPC/APOE2 and BPC/APOE4 mice that are treated with one of the aforementioned translation inhibitors versus a vehicle control.

6.3 APOE2/LRP1 Axis

I identified the APOE receptor LRP1 as necessary for the pro-tumorigenic and pro-metastatic activity of APOE2. Deletion of tumoral *Lrp1* abrogated differences in tumor growth, metastasis, and protein synthesis between *APOE2* and *APOE4* mice. LRP1 is a well-established regulator of intracellular signaling (Boucher and Herz, 2011), thus making it suitable for mediating signals that could impact protein synthesis. Indeed, LRP1 has been shown to regulate PI3K/AKT signaling in glial stem

cells, neurons, adipocytes, and macrophages (Fuentealba et al., 2009; Luo et al., 2018; Safina et al., 2016; Woldt et al., 2011). However, it is somewhat surprising that APOE2 was observed herein to act in a gain-of-function manner via LRP1, as it has been shown to bind to LRP1 approximately 60% less efficiently than APOE3 and APOE4 (Kowal et al., 1990). This calls into question whether APOE2 may be enhancing translation via changes in LRP1 receptor signaling, as APOE has been shown to activate neuronal signaling, including AKT phosphorylation, in an APOE4>APOE3>APOE2 order of potency (Huang *et al.*, 2019). One possible explanation for why APOE2 may nonetheless mediate these effects despite its reduced receptor binding is feedback-induced dosage compensation, as human serum APOE levels follow an APOE2>APOE3>APOE4 order (Li et al., 2020). Another possible explanation could be changes in cellular cholesterol homeostasis, as APOE2 has been shown to be the most efficient cholesterol acceptor of the three variants (Li *et al.*, 2020). Cholesterol efflux can alter the composition of lipid rafts, which have been shown to be critical for LRP1 signaling (Laudati et al., 2016). Future studies will be needed to elucidate the molecular mechanisms downstream of this APOE2/LRP1 axis, as they may reveal new therapeutic targets for the treatment of both Alzheimer's disease and melanoma. This could be approached in an unbiased manner by performing phosphoproteomics of APOE2 and APOE4-expressing melanoma cell lines or tumors with and without LRP1 to determine LRP1-dependent changes in cellular signaling. One could also assay for differences in LRP1 lipid raft partitioning in melanoma cell lines expressing each of the three APOE

variants. Such functional experiments would also help further cement a causal link between APOE2-mediated upregulation of protein synthesis with more aggressive melanoma progressive.

6.4 Implications for Alzheimer's disease

Despite nearly 30 years of research following the discovery that *APOE* genotype impacts Alzheimer's disease risk, the molecular mechanisms underlying this link remain elusive (Belloy *et al.*, 2019). This is a product of the pronounced complexity of APOE, which exhibits diverse roles in numerous biological processes including lipid metabolism, immunity, mitochondrial function, and neuronal repair (Belloy *et al.*, 2019; Huang and Mahley, 2014). The biology behind the protective effect of APOE2 in Alzheimer's has been the most mysterious, partly because there has been substantially less research into its role compared to APOE4 (Suri *et al.*, 2013). It is known that *APOE2* carriers exhibit less cerebral amyloid beta deposition than *APOE3* homozygotes, and APOE2 has been shown experimentally to be more efficient at promoting amyloid beta clearance and degradation than the other variants (Li et al., 2020). However, amyloid beta-independent processes also contribute to the development of Alzheimer's. It has also been unclear whether the *APOE* alleles represent a progressive gain or loss of function of the APOE protein (Belloy et al., 2019). Our work supports the notion that *APOE2* can act as a gain-of-function allele to enhance protein synthesis in a disease context, which has implications for its ability to reduce the risk of Alzheimer's disease.

Supporting the idea that my findings may have broader disease implications, two previously published transcriptomic and proteomic Alzheimer's datasets show that mRNA translation is a pathway that is upregulated in the brains of *APOE2* carriers relative to those of *APOE3* homozygotes and *APOE4* carriers, though translational deregulation was not explored in these studies (Dai et al., 2018; Lefterov et al., 2019). Neuronal protein synthesis has been well established as crucial for synaptic function and memory formation, and it is notably dysregulated in Alzheimer's (Buffington et al., 2014; Hernandez and Abel, 2008). Thus, enhancement of translation may contribute to the protective effect of APOE2 in Alzheimer's and may partly explain the inverse impact of APOE2 and APOE4 variants in melanoma versus Alzheimer's disease. Indeed, additional mechanistic connections between melanoma and Alzheimer's disease are being increasingly uncovered. Recent studies have shown that melanoma cell secretion of amyloid promotes metastasis and is required for survival in the brain (Kleffman et al., 2022; Matafora et al., 2020). It would be worthwhile to validate my findings in Alzheimer's models. This could be first approached by performing the SUnSET assay in induced pluripotent stem cell-derived neurons expressing each of the three human APOE variants (Brookhouser et al., 2021; Lin et al., 2018) to determine if there are differences in puromycin incorporation similar to what I observe in melanoma cells.

6.5 Conclusion

APOE is a potent suppressor of melanoma progression via its effects on invasion, angiogenesis, and anti-tumor immunity. Genetic variation in the *APOE* gene dictates melanoma outcome, as *APOE4* carriers exhibit improved survival and immunotherapy responses compared to *APOE3* homozygotes and *APOE2* carriers, who experience the worst survival. By using a genetically engineered mouse model of melanoma expressing each of the human APOE variants, I have expanded our understanding of this phenomenon by identifying protein synthesis as an oncogenic process that is enhanced by APOE2. Thus, in contrast to the anti-tumor effects of the APOE3 and APOE4 variants, APOE2 is a promoter of melanoma progression. My findings reveal a novel function of APOE2 that may have implications for its protective effect in Alzheimer's disease. My results also provide further support for the use of *APOE* genotype as a biomarker for melanoma outcome and reveal protein synthesis as a potential therapeutic vulnerability in melanoma.

MATERIALS AND METHODS

Mice

Humanized *APOE2* (#1547, C57BL/6NTac), *APOE3* (#1548, C57BL/6), and *APOE4* (#1549, C57BL/6NTac) knock-in mice were obtained from Taconic Biosciences. *Braf*$^{V600E/+}$*;Pten*$^{-/-}$*;Tyr::CreER* (BPC) mice (RRID:IMSR_JAX:013590, C57BL/6J) were obtained from The Jackson Laboratory. *Lrp1*$^{flox/flox}$ mice (C57BL/6J) were generously provided by David Hui (Basford et al., 2011). BPC mice were crossed with *APOE* knock-in mice to generate BPC/APOE2, BPC/APOE3, and BPC/APOE4 mice. BPC/APOE2 and BPC/APOE4 mice were crossed with *Lrp1*$^{flox/flox}$ mice to generate BPC/APOE2/LRP1Δ and BPC/APOE4/LRP1Δ mice. Crosses were maintained on a C57BL/6J background.

Mouse genotyping

Genotyping of *Braf*$^{V600E/+}$*;Pten*$^{-/-}$*;Tyr::CreER* mice was performed as instructed by The Jackson Laboratory. Genotyping for *Lrp1*$^{flox/flox}$ and discernment between mouse (200 bp) and human (~600 bp) *APOE* was performed using standard PCR protocols. To distinguish between human *APOE* alleles, restriction fragment length polymorphism (RFLP) genotyping was performed (Zivelin et al., 1997). Briefly, a 244 bp portion of *APOE* was amplified using standard PCR protocols and digested simultaneously with AflIII (R0541) and HaeII (R0107) restriction enzymes (New England Biolabs) for at least two hours at 37°C. Allele-specific banding was visualized on a 4% agarose gel. The following PCR primers were utilized:

Braf $^{V600E/+}$;Pten$^{fl/fl-}$;Tyr::CreER genetic model

Cre transgene forward: 5’ – GCG GTC TGG CAG TAA AAA CTA TC – 3’

Cre transgene reverse: 5’ – GTG AAA CAG CAT TGC TGT CAC TT – 3’

Cre internal control forward: 5’ – CAC GTG GGC TCC AGC ATT – 3’

Cre internal control reverse: 5’ – TCA CCA GTC ATT TCT GCC TTT G – 3’

Braf forward: 5’ – TGA GTA TTT TTG TGG CAA CTG C – 3’

Braf reverse: 5’ – CTC TGC TGG GAA AGC GGC – 3’

Pten forward: 5’ – CAA GCA CTC TGC GAA CTG AG – 3’

Pten reverse: 5’ – AAG TTT TTG AAG GCA AGA TGC – 3’

Mouse versus human APOE

Common forward: 5’ – TAC CGG CTC AAC TAG GAA CCA T – 3’

Mouse Apoe reverse: 5’ – TTT AAT CGT CCT CCA TCC CTG C – 3’

Human APOE reverse: 5’ – GTT CCA TCT CAG TCC CAG TCTC – 3’

Human APOE allele RFLP

Human APOE forward: 5’ – ACA GAA TTC GCC CCG GCC TGG TAC AC – 3’

Human APOE reverse: 5’ – TAA GCT TGG CAC GGC TGT CCA AGG A – 3’

Lrp1$^{flox/flox}$

Lrp1 forward: 5’ – CAT ACC CTC TTC AAA CCC CTT CCT G – 3’

Lrp1 reverse: 5' – GCA AGC TCT CCT GCT CAG ACC TGG A – 3'

Cell lines

HEK293T cells were obtained from the American Tissue Type Collection (ATCC). The B16F10 cell line transduced with a retroviral construct to express luciferase and GFP (Ponomarev et al., 2004) and short hairpin RNA (shRNA) targeting murine *Apoe* (Millipore Sigma, TRCN0000011799; B16F10-TR-sh*Apoe*) was previously described (Ostendorf *et al.*, 2020; Pencheva *et al.*, 2014). B16F10-TR-sh*Apoe* and HEK293T cells were cultured in DMEM (Gibco, 11995) supplemented with 10% fetal bovine serum (FBS) (D10F). All cells were maintained in an incubator at 37°C and 5% CO_2 and regularly tested for *Mycoplasma* contamination with the Universal Mycoplasma Detection Kit (ATCC, 30-1012K).

Generation of stable cell lines

APOE coding sequences from pCMV4-APOE2 (RRID:Addgene_87085), pCMV4-APOE3 (RRID:Addgene_87086), and pCMV4-APOE4 (RRID:Addgene_87087) plasmids were subcloned into the pBabe-hygro vector (RRID:Addgene_1765). Retrovirus was produced in HEK293T cells grown in 10 cm plates. Cells were transfected with retroviral Gag-pol (8 ug) and VSV-G (4 ug) packaging plasmids and pBabe vector (8 ug) using PEI Max transfection reagent (VWR, 75800-188). After 24 h, the medium was replaced with fresh DF10, and virus-containing supernatant was collected 48 and 72 h after transfection. The

supernatant was filtered through a 0.45 µm filter, and viral supernatant was used with 8 µg/ml polybrene (Sigma, TR-1003-G) to transduce pre-plated B16F10-TR-sh*Apoe* cells for 8 hours. Following a second round of transduction, antibiotic selection was performed using 600 µg/ml Hygromycin B (Invitrogen, 10687010). Protein overexpression was validated by western blot.

Generation of CRISPR cell lines

Single guide RNA sequences targeting murine *Lrp1* were obtained from the GeCKO v2 library (Sanjana et al., 2014) and cloned into the pSpCas(BB)-2A-Puro (PX459) V2.0 vector (RRID:Addgene_62988). B16F10-TR-sh*Apoe* cells were plated into a 6-well dish the day prior to transfection and transfected with 4 µg plasmid and TurboFect transfection reagent (Thermo Scientific, R0533) diluted in serum-free media, according to the manufacturer's instructions. 24 hours after transfection, puromycin selection was initiated at 2 µg/mL concentration (Thermo Scientific, A1113803). Single clones were obtained by limiting dilution followed by Sanger sequencing of individual clones to confirm the presence of indels. Knockout clones were pooled to reconstitute heterogeneity, and LRP1 knockout was confirmed via western blot.

Guide RNA sequences:

sgCtrl: 5' – GCGAGGTATTCGGCTCCGCG – 3'

sg*Lrp1*-1: 5' – CCCGTTGCAGAGACGAGACA – 3'

sg*Lrp1*-2: 5’ – TTTGACGAGTGTTCCGTGTA – 3’

Tail vein metastasis assay

6–8-week-old male *APOE2* and *APOE4* knock-in mice were injected via lateral tail vein with 100 µl of PBS containing 1×10^5 B16F10-TR-sh*Apoe* cells. D-luciferin (GoldBio, 115144-35-9) was injected retro-orbitally, and bioluminescence was measured with an IVIS Lumina II (Caliper Life Sciences). Bioluminescence imaging was performed weekly, and signal was normalized to the signal obtained on day 0.

Histology

Mice were perfused via intracardiac injection with PBS followed by 4% paraformaldehyde (PFA). The lungs were resected, incubated in 4% paraformaldehyde at 4°C overnight, and dehydrated in 70% ethanol at 4°C. Lungs were then embedded in paraffin, cut into 5 µm sections, and stained with hematoxylin and eosin (Histoserv, Inc.). Slides were digitally scanned with a PathScan Enabler (Meyer Instruments).

Genetic tumor initiation

Topical induction

10 mg/ml of 4-hydroxytamoxifen (4-OHT; Sigma, H6278) was dissolved in acetone with gentle heating. 6–8-week-old female mice were shaved on the back,

and 5 µl of 4-OHT was applied to back skin and allowed to air dry. Mice were observed twice weekly for tumor formation, defined as a raised, pigmented lesion at the site of tamoxifen application. Tumor volume was measured as described previously (Spranger et al., 2015) by assessing length, width and height using a digital caliper ($V=l \times w \times h$), as tumors tended to grow cuboidal rather than spherical. For survival analyses, mice were euthanized according to the humane endpoints outlined in the IACUC protocol.

Perinatal induction

Two-day-old female neonates were tail snipped as described previously (Westmark et al., 2021) and genotyped. 10 µl of 4-OHT diluted in DMSO (50 mg/mL) was applied with a small paintbrush to the back skin of neonates on postnatal days 3, 5, and 7. Mice were euthanized on postnatal day 35 or when moribund, whichever occurred earlier.

Immunofluorescence of BPC tumor sections

Fresh tumors were excised, embedded in optimal cutting temperature (OCT) compound (Sakura Finetek, 4583), flash frozen in liquid nitrogen, and stored at -80°C. 20 µM tumor sections were obtained with a cryostat. Sections were fixed at -20°C with acetone/methanol and permeabilized with 0.1% Triton-X for 10 minutes at room temperature (RT). Blocking was performed for 30 minutes at RT with 5% goat serum in PBS with 0.1% Tween 20 (PBST). Sections were incubated at 4°C

overnight with LRP1 primary antibody diluted in blocking solution (1:100; abcam 92544). Slides were washed with PBS and then incubated with Alexa Fluor 488 anti-rabbit secondary antibody diluted in PBST for 45 minutes (1:200; Invitrogen A11008). Slides were washed again with PBS, and nuclei were stained with 1 μg/mL of DAPI (Roche, 10236276001) followed by mounting with ProLong Gold Antifade Mountant (Invitrogen, P36930). Four independent fields per tumor section were imaged at random with a Nikon A1R MP confocal microscope with consistent instrument settings between samples. Sections stained with secondary antibody alone were used as negative controls.

Quantification of BPC lung metastases

Lungs were fixed and dehydrated as described above. Lungs were then visualized with an OMAX trinocular microscope (W43C1-L08-TP). The number of pigmented lesions on the surface of each lung was quantified in a blinded manner under high magnification.

Western blot

Cells were lysed in ice cold RIPA buffer (G-Biosciences, 786-490) supplemented with protease inhibitor cocktail (Roche, 11836153001). Samples were denatured, separated by SDS-PAGE with 4-12% Bis-tris gels (Sigma), and transferred to low fluorescence PVDF membranes with the Trans-Blot Turbo Transfer System according to manufacturer's instructions (Bio-Rad). Membranes

were blocked for one hour with Intercept Blocking Buffer (LI-COR, 927-7000) and probed overnight at 4°C with the following primary antibodies diluted in blocking buffer containing 0.2% Tween-20: Puromycin (1:10000, Millipore #MABE343), APOE (1:1000, GeneTex #GTX100053), HSC70 (1:1000, Santa Cruz #sc-7298), LRP1 (1:50000, abcam #92544). Membranes were washed with PBST and incubated for an hour with IRDye 680RD goat anti-mouse (926-68070) or 800CW goat anti-rabbit (926-32211) secondary antibodies diluted in blocking buffer containing 0.2% Tween 20 and 0.1% SDS (LI-COR). Blots were imaged and analyzed with Image Studio Lite and Empiria Studio software (LI-COR).

SUnSET assay

In Vivo

BPC tumors were topically induced in mice as described above. 35 days after induction, mice were weighed and injected intraperitoneally with 40 nmol/g of puromycin. Mice were placed back in their cage for 30 minutes, after which mice were anesthetized with isoflurane and sacrificed by cervical dislocation. Tumors were dissected and rinsed with PBS to remove blood. ~10mg of tumor was dissected from the center of tumors and homogenized with a Bead Ruptor Elite (Omni International) at 0°C in 200 µL of RIPA supplemented with protease inhibitor cocktail. To reduce viscosity, lysates were then treated with DNAse I (Norgen, 25710) according to manufacturer's instructions. 40 µg of lysate was loaded and western blot was run and analyzed as described above. A mouse IgG2a-specific

secondary antibody (1:5000; LI-COR, 926-32351) was used to eliminate background mouse IgG signal. Total protein was detected with the Revert 700 Total Protein Staining kit (LI-COR, 926-11010).

In Vitro

$5x10^4$ B16F10-TR-sh*Apoe* cells stably expressing APOE2, APOE3, APOE4, or empty vector were plated in 8-well chamber slides (Nunc, 154941) the day before experiment. The next day, cells were serum starved for 6 hours in DMEM containing 0.2% FBS and then stimulated for 15 minutes with DF10. After stimulation, cells were pulsed with 10 µg/mL puromycin in DF10 for 30 minutes. As a positive control, one group of cells was treated with 100 µg/mL CHX for 10 minutes in DF10 prior to puromycin treatment. Cells were washed twice with PBS and then fixed with 4% PFA for 10 minutes. Cells were washed twice with PBS for 5 minutes each and then permeabilized with 0.5% Triton X-100 for 10 minutes. Two 5-minute PBS washes were performed, and cells were then incubated for 90 minutes at RT with 0.1% Triton X-100 containing Alexa Fluor 647-conjugated anti-puromycin antibody (1:5000; Millipore, MABE343-AF647). Cells were washed thrice with PBST for 5 minutes each. During the second wash, DAPI was added at a 1 µg/mL concentration. Slides were mounted with ProLong Gold and left to dry overnight. Four independent fields per condition were imaged at random with a Nikon A1R MP confocal microscope with consistent instrument settings between conditions. Mean fluorescence intensity was quantified with ImageJ.

RNA extraction from BPC tumors

Primary tumors were dissected 49 days after 4-OHT administration, flash frozen in liquid nitrogen, and stored at -80°C until RNA extraction. For RNA extraction, 10mg of tissue was dissected from the center of tumors on a ThermalTray (Corning, 432074) placed on dry ice. Tumor pieces were placed in homogenizer tubes containing ceramic beads along with lysis buffer from the Total RNA Purification Kit (Norgen, 37500) and RNAse inhibitors (10 µl/mL β-mercaptoethanol and 200 units/mL RNAsin Plus (Promega, N2615)), flash frozen in liquid nitrogen, and homogenized with a Bead Ruptor Elite at 0°C. RNA was then purified with the Total RNA Purification Kit with on-column DNAse treatment per manufacturer's instructions.

RNA-Seq

RNA integrity numbers (RIN) were measured with an Agilent Bioanalyzer 2100, with an average RIN of 8.15. TruSeq RNA Library Prep Kit v2, Set A (Illumina, RS-122-2001) was used to generate RNA-seq libraries according to manufacturer's instructions. Libraries were quantified with an Agilent TapeStation and pooled at equimolar concentrations. Pooled libraries were sequenced with an Illumina NextSeq 500 (High Output, 75 SR). For analysis, FASTQ file quality was checked with FastQC (https://www.bioinformatics.babraham.ac.uk/projects/fastqc/). Kallisto v0.46.1 (Bray et al., 2016) was used to pseudoalign reads to the mm10 mouse

transcriptome (version 101) downloaded from Ensembl. Quality data was aggregated with MultiQC (Ewels et al., 2016). Counts were imported into R v4.1.3. with RStudio v2022.02.1 and tximport v1.18.0 (Soneson et al., 2015). Differential expression analysis was performed with DESeq2 v1.28.1 (Love et al., 2014) after prefiltering genes with less than 10 counts. Genes were annotated with AnnotationDbi v1.52.0 and the org.Mm.eg.db package. Genes were ranked based on Wald statistic, and GSEA was performed with the fgsea v1.20.0 (Korotkevich et al., 2021). Mouse gene sets were downloaded from http://bioinf.wehi.edu.au/MSigDB/ based on MSigDB v7.1.

TCGA analysis

Harmonized raw counts of tumor transcriptomes from the TCGA-SKCM study were downloaded from the Genomic Data Commons API and imported into R with TCGAbiolinks v2.18.0 (Colaprico et al., 2016). *APOE* genotype information from whole exome sequencing was utilized as determined previously (Ostendorf *et al.*, 2020). Differential expression analysis was performed as described for BPC tumors, with tumor stage included as a covariate for primary tumor analysis to account for differences in tumor progression between genotypes. Genes were annotated with AnnotationDbi v1.52.0 and the org.Hs.eg.db package. The Reactome gene set was downloaded from MSigDB v7.1, and GSEA was performed as described above.

Statistical analysis

All data are expressed as mean ± SEM, unless indicated otherwise. Groups were compared using statistical tests for significance as described in the figure legends. A P value less than 0.05 was considered statistically significant. Statistical tests were performed with GraphPad Prism 9.

Schematics in this thesis were generated with BioRender.com.

REFERENCES

American Cancer Society (2022). Cancer Facts & Figures 2022. American Cancer Society.

Balch, C.M., Atkins, M.B., Garbe, C., Gershenwald, J.E., Halpern, A.C., Kirkwood, J.M., McArthur, G.A., Thompson, J.F., Sober, A.J., and SpringerLink. (2020). Cutaneous Melanoma, 6th 2020. Edition (Springer International Publishing : Imprint: Springer).

Basford, J.E., Wancata, L., Hofmann, S.M., Silva, R.A., Davidson, W.S., Howles, P.N., and Hui, D.Y. (2011). Hepatic deficiency of low density lipoprotein receptor-related protein-1 reduces high density lipoprotein secretion and plasma levels in mice. J Biol Chem *286*, 13079-13087. 10.1074/jbc.M111.229369.

Belloy, M.E., Napolioni, V., and Greicius, M.D. (2019). A Quarter Century of APOE and Alzheimer's Disease: Progress to Date and the Path Forward. Neuron *101*, 820-838. 10.1016/j.neuron.2019.01.056.

Bohnet, K., Pillot, T., Visvikis, S., Sabolovic, N., and Siest, G. (1996). Apolipoprotein (apo) E genotype and apoE concentration determine binding of normal very low density lipoproteins to HepG2 cell surface receptors. J Lipid Res *37*, 1316-1324.

Boucher, P., and Herz, J. (2011). Signaling through LRP1: Protection from atherosclerosis and beyond. Biochem Pharmacol *81*, 1-5. 10.1016/j.bcp.2010.09.018.

Boulagnon-Rombi, C., Schneider, C., Leandri, C., Jeanne, A., Grybek, V., Bressenot, A.M., Barbe, C., Marquet, B., Nasri, S., Coquelet, C., et al. (2018). LRP1 expression in colon cancer predicts clinical outcome. Oncotarget *9*, 8849-8869. 10.18632/oncotarget.24225.

Bray, N.L., Pimentel, H., Melsted, P., and Pachter, L. (2016). Near-optimal probabilistic RNA-seq quantification. Nat Biotechnol *34*, 525-527. 10.1038/nbt.3519.

Brookhouser, N., Raman, S., Frisch, C., Srinivasan, G., and Brafman, D.A. (2021). APOE2 mitigates disease-related phenotypes in an isogenic hiPSC-based model of Alzheimer's disease. Mol Psychiatry *26*, 5715-5732. 10.1038/s41380-021-01076-3.

Buffington, S.A., Huang, W., and Costa-Mattioli, M. (2014). Translational control in synaptic plasticity and cognitive dysfunction. Annu Rev Neurosci *37*, 17-38. 10.1146/annurev-neuro-071013-014100.

Butler, T.P., and Gullino, P.M. (1975). Quantitation of cell shedding into efferent blood of mammary adenocarcinoma. Cancer Res *35*, 512-516.

Cancer Genome Atlas Network (2015). Genomic Classification of Cutaneous Melanoma. Cell *161*, 1681-1696. 10.1016/j.cell.2015.05.044.

Celia-Terrassa, T., and Kang, Y. (2016). Distinctive properties of metastasis-initiating cells. Genes Dev *30*, 892-908. 10.1101/gad.277681.116.

Chen, J., Li, Q., and Wang, J. (2011). Topology of human apolipoprotein E3 uniquely regulates its diverse biological functions. Proc Natl Acad Sci U S A *108*, 14813-14818. 10.1073/pnas.1106420108.

Clark, W.H., Jr., Elder, D.E., Guerry, D.t., Epstein, M.N., Greene, M.H., and Van Horn, M. (1984). A study of tumor progression: the precursor lesions of superficial spreading and nodular melanoma. Hum Pathol *15*, 1147-1165. 10.1016/s0046-8177(84)80310-x.

Colaprico, A., Silva, T.C., Olsen, C., Garofano, L., Cava, C., Garolini, D., Sabedot, T.S., Malta, T.M., Pagnotta, S.M., Castiglioni, I., et al. (2016). TCGAbiolinks: an R/Bioconductor package for integrative analysis of TCGA data. Nucleic Acids Res *44*, e71. 10.1093/nar/gkv1507.

Conciatori, F., Ciuffreda, L., Bazzichetto, C., Falcone, I., Pilotto, S., Bria, E., Cognetti, F., and Milella, M. (2018). mTOR Cross-Talk in Cancer and Potential for Combination Therapy. Cancers (Basel) *10*. 10.3390/cancers10010023.

Corbo, R.M., and Scacchi, R. (1999). Apolipoprotein E (APOE) allele distribution in the world. Is APOE*4 a 'thrifty' allele? Ann Hum Genet *63*, 301-310. 10.1046/j.1469-1809.1999.6340301.x.

Corder, E.H., Saunders, A.M., Risch, N.J., Strittmatter, W.J., Schmechel, D.E., Gaskell, P.C., Jr., Rimmler, J.B., Locke, P.A., Conneally, P.M., Schmader, K.E., and et al. (1994). Protective effect of apolipoprotein E type 2 allele for late onset Alzheimer disease. Nat Genet *7*, 180-184. 10.1038/ng0694-180.

Dai, J., Johnson, E.C.B., Dammer, E.B., Duong, D.M., Gearing, M., Lah, J.J., Levey, A.I., Wingo, T.S., and Seyfried, N.T. (2018). Effects of APOE Genotype on Brain Proteomic Network and Cell Type Changes in Alzheimer's Disease. Front Mol Neurosci *11*, 454. 10.3389/fnmol.2018.00454.

Damsky, W.E., Curley, D.P., Santhanakrishnan, M., Rosenbaum, L.E., Platt, J.T., Gould Rothberg, B.E., Taketo, M.M., Dankort, D., Rimm, D.L., McMahon, M., and Bosenberg, M. (2011). beta-catenin signaling controls metastasis in Braf-activated Pten-deficient melanomas. Cancer Cell *20*, 741-754. 10.1016/j.ccr.2011.10.030.

Damsky, W.E., Rosenbaum, L.E., and Bosenberg, M. (2010). Decoding melanoma metastasis. Cancers (Basel) *3*, 126-163. 10.3390/cancers3010126.

Damsky, W.E., Theodosakis, N., and Bosenberg, M. (2014). Melanoma metastasis: new concepts and evolving paradigms. Oncogene *33*, 2413-2422. 10.1038/onc.2013.194.

Dankort, D., Curley, D.P., Cartlidge, R.A., Nelson, B., Karnezis, A.N., Damsky, W.E., Jr., You, M.J., DePinho, R.A., McMahon, M., and Bosenberg, M. (2009). Braf(V600E) cooperates with Pten loss to induce metastatic melanoma. Nat Genet *41*, 544-552. 10.1038/ng.356.

Davis, E.J., Johnson, D.B., Sosman, J.A., and Chandra, S. (2018). Melanoma: What do all the mutations mean? Cancer *124*, 3490-3499. 10.1002/cncr.31345.

Dedieu, S., Langlois, B., Devy, J., Sid, B., Henriet, P., Sartelet, H., Bellon, G., Emonard, H., and Martiny, L. (2008). LRP-1 silencing prevents malignant cell invasion despite increased pericellular proteolytic activities. Mol Cell Biol *28*, 2980-2995. 10.1128/MCB.02238-07.

Domingues, B., Lopes, J.M., Soares, P., and Populo, H. (2018). Melanoma treatment in review. Immunotargets Ther *7*, 35-49. 10.2147/ITT.S134842.

Ewels, P., Magnusson, M., Lundin, S., and Kaller, M. (2016). MultiQC: summarize analysis results for multiple tools and samples in a single report. Bioinformatics *32*, 3047-3048. 10.1093/bioinformatics/btw354.

Farrer, L.A., Cupples, L.A., Haines, J.L., Hyman, B., Kukull, W.A., Mayeux, R., Myers, R.H., Pericak-Vance, M.A., Risch, N., and van Duijn, C.M. (1997). Effects of age, sex, and ethnicity on the association between apolipoprotein E genotype and Alzheimer disease. A meta-analysis. APOE and Alzheimer Disease Meta Analysis Consortium. JAMA *278*, 1349-1356.

Fayard, B., Bianchi, F., Dey, J., Moreno, E., Djaffer, S., Hynes, N.E., and Monard, D. (2009). The serine protease inhibitor protease nexin-1 controls mammary cancer metastasis through LRP-1-mediated MMP-9 expression. Cancer Res *69*, 5690-5698. 10.1158/0008-5472.CAN-08-4573.

Fidler, I.J. (1970). Metastasis: quantitative analysis of distribution and fate of tumor emboli labeled with 125 I-5-iodo-2'-deoxyuridine. J Natl Cancer Inst *45*, 773-782.
Font-Clos, F., Zapperi, S., and La Porta, C.A.M. (2020). Blood Flow Contributions to Cancer Metastasis. iScience *23*, 101073. 10.1016/j.isci.2020.101073.

Fuentealba, R.A., Liu, Q., Kanekiyo, T., Zhang, J., and Bu, G. (2009). Low density lipoprotein receptor-related protein 1 promotes anti-apoptotic signaling in neurons by activating Akt survival pathway. J Biol Chem *284*, 34045-34053. 10.1074/jbc.M109.021030.

Gandhi, V., Plunkett, W., and Cortes, J.E. (2014). Omacetaxine: a protein translation inhibitor for treatment of chronic myelogenous leukemia. Clin Cancer Res *20*, 1735-1740. 10.1158/1078-0432.CCR-13-1283.

Geller, A.C., Clapp, R.W., Sober, A.J., Gonsalves, L., Mueller, L., Christiansen, C.L., Shaikh, W., and Miller, D.R. (2013). Melanoma epidemic: an analysis of six decades of data from the Connecticut Tumor Registry. J Clin Oncol *31*, 4172-4178. 10.1200/JCO.2012.47.3728.

Glasziou, P.P., Jones, M.A., Pathirana, T., Barratt, A.L., and Bell, K.J. (2020). Estimating the magnitude of cancer overdiagnosis in Australia. Med J Aust *212*, 163-168. 10.5694/mja2.50455.

Gonias, S.L., and Campana, W.M. (2014). LDL receptor-related protein-1: a regulator of inflammation in atherosclerosis, cancer, and injury to the nervous system. Am J Pathol *184*, 18-27. 10.1016/j.ajpath.2013.08.029.

Goodman, C.A., and Hornberger, T.A. (2013). Measuring protein synthesis with SUnSET: a valid alternative to traditional techniques? Exerc Sport Sci Rev *41*, 107-115. 10.1097/JES.0b013e3182798a95.

Guttman, M., Betts, G.N., Barnes, H., Ghassemian, M., van der Geer, P., and Komives, E.A. (2009). Interactions of the NPXY microdomains of the low density lipoprotein receptor-related protein 1. Proteomics *9*, 5016-5028. 10.1002/pmic.200900457.
Hernandez, P.J., and Abel, T. (2008). The role of protein synthesis in memory consolidation: progress amid decades of debate. Neurobiol Learn Mem *89*, 293-311. 10.1016/j.nlm.2007.09.010.

Herz, J., Hamann, U., Rogne, S., Myklebost, O., Gausepohl, H., and Stanley, K.K. (1988). Surface location and high affinity for calcium of a 500-kd liver membrane protein closely related to the LDL-receptor suggest a physiological role as lipoprotein receptor. EMBO J *7*, 4119-4127.

Herz, J., and Strickland, D.K. (2001). LRP: a multifunctional scavenger and signaling receptor. J Clin Invest *108*, 779-784. 10.1172/JCI13992.

Hodis, E., Watson, I.R., Kryukov, G.V., Arold, S.T., Imielinski, M., Theurillat, J.P., Nickerson, E., Auclair, D., Li, L., Place, C., et al. (2012). A landscape of driver mutations in melanoma. Cell *150*, 251-263. 10.1016/j.cell.2012.06.024.

Huang, Y., and Mahley, R.W. (2014). Apolipoprotein E: structure and function in lipid metabolism, neurobiology, and Alzheimer's diseases. Neurobiol Dis *72 Pt A*, 3-12. 10.1016/j.nbd.2014.08.025.

Huang, Y.A., Zhou, B., Nabet, A.M., Wernig, M., and Sudhof, T.C. (2019). Differential Signaling Mediated by ApoE2, ApoE3, and ApoE4 in Human Neurons Parallels Alzheimer's Disease Risk. J Neurosci *39*, 7408-7427. 10.1523/JNEUROSCI.2994-18.2019.

Huang, Y.A., Zhou, B., Wernig, M., and Sudhof, T.C. (2017). ApoE2, ApoE3, and ApoE4 Differentially Stimulate APP Transcription and Abeta Secretion. Cell *168*, 427-441 e421. 10.1016/j.cell.2016.12.044.

Huebbe, P., and Rimbach, G. (2017). Evolution of human apolipoprotein E (APOE) isoforms: Gene structure, protein function and interaction with dietary factors. Ageing Res Rev *37*, 146-161. 10.1016/j.arr.2017.06.002.

Jassal, B., Matthews, L., Viteri, G., Gong, C., Lorente, P., Fabregat, A., Sidiropoulos, K., Cook, J., Gillespie, M., Haw, R., et al. (2019). The reactome pathway knowledgebase. Nucleic Acids Research *48*, D498-D503. 10.1093/nar/gkz1031.

Kaplan, R.N., Riba, R.D., Zacharoulis, S., Bramley, A.H., Vincent, L., Costa, C., MacDonald, D.D., Jin, D.K., Shido, K., Kerns, S.A., et al. (2005). VEGFR1-positive haematopoietic bone marrow progenitors initiate the pre-metastatic niche. Nature *438*, 820-827. 10.1038/nature04186.

Kleffman, K., Levinson, G., Rose, I.V.L., Blumenberg, L.M., Shadaloey, S.A.A., Dhabaria, A., Wong, E., Galan-Echevarria, F., Karz, A., Argibay, D., et al. (2022). Melanoma-Secreted Amyloid Beta Suppresses Neuroinflammation and Promotes Brain Metastasis. Cancer Discov *12*, 1314-1335. 10.1158/2159-8290.CD-21-1006.

Knouff, C., Hinsdale, M.E., Mezdour, H., Altenburg, M.K., Watanabe, M., Quarfordt, S.H., Sullivan, P.M., and Maeda, N. (1999). Apo E structure determines VLDL clearance and atherosclerosis risk in mice. J Clin Invest *103*, 1579-1586. 10.1172/JCI6172.

Kockx, M., Traini, M., and Kritharides, L. (2018). Cell-specific production, secretion, and function of apolipoprotein E. J Mol Med (Berl) *96*, 361-371. 10.1007/s00109-018-1632-y.

Korotkevich, G., Sukhov, V., Budin, N., Shpak, B., Artyomov, M.N., and Sergushichev, A. (2021). Fast gene set enrichment analysis. bioRxiv, 060012. 10.1101/060012.

Kowal, R.C., Herz, J., Weisgraber, K.H., Mahley, R.W., Brown, M.S., and Goldstein, J.L. (1990). Opposing effects of apolipoproteins E and C on lipoprotein binding to low density lipoprotein receptor-related protein. J Biol Chem *265*, 10771-10779.

Lane-Donovan, C., and Herz, J. (2017). ApoE, ApoE Receptors, and the Synapse in Alzheimer's Disease. Trends Endocrinol Metab *28*, 273-284. 10.1016/j.tem.2016.12.001.

Langlois, B., Perrot, G., Schneider, C., Henriet, P., Emonard, H., Martiny, L., and Dedieu, S. (2010). LRP-1 promotes cancer cell invasion by supporting ERK and inhibiting JNK signaling pathways. PLoS One *5*, e11584. 10.1371/journal.pone.0011584.

Larkin, J., Chiarion-Sileni, V., Gonzalez, R., Grob, J.J., Rutkowski, P., Lao, C.D., Cowey, C.L., Schadendorf, D., Wagstaff, J., Dummer, R., et al. (2019). Five-Year Survival with Combined Nivolumab and Ipilimumab in Advanced Melanoma. N Engl J Med *381*, 1535-1546. 10.1056/NEJMoa1910836.

Laudati, E., Gilder, A.S., Lam, M.S., Misasi, R., Sorice, M., Gonias, S.L., and Mantuano, E. (2016). The activities of LDL Receptor-related Protein-1 (LRP1) compartmentalize into distinct plasma membrane microdomains. Mol Cell Neurosci *76*, 42-51. 10.1016/j.mcn.2016.08.006.

Lefterov, I., Wolfe, C.M., Fitz, N.F., Nam, K.N., Letronne, F., Biedrzycki, R.J., Kofler, J., Han, X., Wang, J., Schug, J., and Koldamova, R. (2019). APOE2 orchestrated differences in transcriptomic and lipidomic profiles of postmortem AD brain. Alzheimers Res Ther *11*, 113. 10.1186/s13195-019-0558-0.

Li, Z., Shue, F., Zhao, N., Shinohara, M., and Bu, G. (2020). APOE2: protective mechanism and therapeutic implications for Alzheimer's disease. Mol Neurodegener *15*, 63. 10.1186/s13024-020-00413-4.

Lillis, A.P., Van Duyn, L.B., Murphy-Ullrich, J.E., and Strickland, D.K. (2008). LDL receptor-related protein 1: unique tissue-specific functions revealed by selective gene knockout studies. Physiol Rev *88*, 887-918. 10.1152/physrev.00033.2007.

Lin, Y.T., Seo, J., Gao, F., Feldman, H.M., Wen, H.L., Penney, J., Cam, H.P., Gjoneska, E., Raja, W.K., Cheng, J., et al. (2018). APOE4 Causes Widespread Molecular and Cellular Alterations Associated with Alzheimer's Disease Phenotypes in Human iPSC-Derived Brain Cell Types. Neuron *98*, 1294. 10.1016/j.neuron.2018.06.011.

Love, M.I., Huber, W., and Anders, S. (2014). Moderated estimation of fold change and dispersion for RNA-seq data with DESeq2. Genome Biol *15*, 550. 10.1186/s13059-014-0550-8.

Luo, L., Wall, A.A., Tong, S.J., Hung, Y., Xiao, Z., Tarique, A.A., Sly, P.D., Fantino, E., Marzolo, M.P., and Stow, J.L. (2018). TLR Crosstalk Activates LRP1 to Recruit Rab8a and PI3Kgamma for Suppression of Inflammatory Responses. Cell Rep *24*, 3033-3044. 10.1016/j.celrep.2018.08.028.

Luzzi, K.J., MacDonald, I.C., Schmidt, E.E., Kerkvliet, N., Morris, V.L., Chambers, A.F., and Groom, A.C. (1998). Multistep nature of metastatic inefficiency: dormancy of solitary cells after successful extravasation and limited survival of early micrometastases. Am J Pathol *153*, 865-873. 10.1016/S0002-9440(10)65628-3.

Mahley, R.W. (2016). Central Nervous System Lipoproteins: ApoE and Regulation of Cholesterol Metabolism. Arterioscler Thromb Vasc Biol *36*, 1305-1315. 10.1161/ATVBAHA.116.307023.

Mahley, R.W., and Huang, Y. (1999). Apolipoprotein E: from atherosclerosis to Alzheimer's disease and beyond. Curr Opin Lipidol *10*, 207-217. 10.1097/00041433-199906000-00003.

Mahley, R.W., and Rall, S.C., Jr. (2000). Apolipoprotein E: far more than a lipid transport protein. Annu Rev Genomics Hum Genet *1*, 507-537. 10.1146/annurev.genom.1.1.507.

Mahley, R.W., Weisgraber, K.H., and Huang, Y. (2009). Apolipoprotein E: structure determines function, from atherosclerosis to Alzheimer's disease to AIDS. J Lipid Res *50 Suppl*, S183-188. 10.1194/jlr.R800069-JLR200.

Martinez-Martinez, A.B., Torres-Perez, E., Devanney, N., Del Moral, R., Johnson, L.A., and Arbones-Mainar, J.M. (2020). Beyond the CNS: The many peripheral roles of APOE. Neurobiol Dis *138*, 104809. 10.1016/j.nbd.2020.104809.

Matafora, V., Farris, F., Restuccia, U., Tamburri, S., Martano, G., Bernardelli, C., Sofia, A., Pisati, F., Casagrande, F., Lazzari, L., et al. (2020). Amyloid aggregates accumulate in melanoma metastasis modulating YAP activity. EMBO Rep *21*, e50446. 10.15252/embr.202050446.

Matthews, N.H., Li, W., Qureshi, A.A., Weinstock, M.A., and Cho, E. (2017). Cutaneous Melanoma: Etiology and Therapy (Codon Publications).

Michaloglou, C., Vredeveld, L.C., Soengas, M.S., Denoyelle, C., Kuilman, T., van der Horst, C.M., Majoor, D.M., Shay, J.W., Mooi, W.J., and Peeper, D.S. (2005). BRAFE600-associated senescence-like cell cycle arrest of human naevi. Nature *436*, 720-724. 10.1038/nature03890.

Miller, A.J., and Mihm, M.C., Jr. (2006). Melanoma. N Engl J Med *355*, 51-65. 10.1056/NEJMra052166.

Montel, V., Gaultier, A., Lester, R.D., Campana, W.M., and Gonias, S.L. (2007). The low-density lipoprotein receptor-related protein regulates cancer cell survival and metastasis development. Cancer Res *67*, 9817-9824. 10.1158/0008-5472.CAN-07-0683.

Muratoglu, S.C., Mikhailenko, I., Newton, C., Migliorini, M., and Strickland, D.K. (2010). Low density lipoprotein receptor-related protein 1 (LRP1) forms a signaling complex with platelet-derived growth factor receptor-beta in endosomes and regulates activation of the MAPK pathway. J Biol Chem *285*, 14308-14317. 10.1074/jbc.M109.046672.

Nakashima, Y., Plump, A.S., Raines, E.W., Breslow, J.L., and Ross, R. (1994). ApoE-deficient mice develop lesions of all phases of atherosclerosis throughout the arterial tree. Arterioscler Thromb *14*, 133-140. 10.1161/01.atv.14.1.133.

Ostendorf, B.N., Bilanovic, J., Adaku, N., Tafreshian, K.N., Tavora, B., Vaughan, R.D., and Tavazoie, S.F. (2020). Common germline variants of the human APOE gene modulate melanoma progression and survival. Nat Med *26*, 1048-1053. 10.1038/s41591-020-0879-3.

Paget, S. (1889). THE DISTRIBUTION OF SECONDARY GROWTHS IN CANCER OF THE BREAST. The Lancet *133*, 571-573. https://doi.org/10.1016/S0140-6736(00)49915-0.

Peinado, H., Zhang, H., Matei, I.R., Costa-Silva, B., Hoshino, A., Rodrigues, G., Psaila, B., Kaplan, R.N., Bromberg, J.F., Kang, Y., et al. (2017). Pre-metastatic niches: organ-specific homes for metastases. Nat Rev Cancer *17*, 302-317. 10.1038/nrc.2017.6.

Pencheva, N., Buss, C.G., Posada, J., Merghoub, T., and Tavazoie, S.F. (2014). Broad-spectrum therapeutic suppression of metastatic melanoma through nuclear hormone receptor activation. Cell *156*, 986-1001. 10.1016/j.cell.2014.01.038.

Pencheva, N., Tran, H., Buss, C., Huh, D., Drobnjak, M., Busam, K., and Tavazoie, S.F. (2012). Convergent multi-miRNA targeting of ApoE drives LRP1/LRP8-dependent melanoma metastasis and angiogenesis. Cell *151*, 1068-1082. 10.1016/j.cell.2012.10.028.

Ponomarev, V., Doubrovin, M., Serganova, I., Vider, J., Shavrin, A., Beresten, T., Ivanova, A., Ageyeva, L., Tourkova, V., Balatoni, J., et al. (2004). A novel triple-modality reporter gene for whole-body fluorescent, bioluminescent, and nuclear

noninvasive imaging. Eur J Nucl Med Mol Imaging *31*, 740-751. 10.1007/s00259-003-1441-5.

Posch, C., Moslehi, H., Feeney, L., Green, G.A., Ebaee, A., Feichtenschlager, V., Chong, K., Peng, L., Dimon, M.T., Phillips, T., et al. (2013). Combined targeting of MEK and PI3K/mTOR effector pathways is necessary to effectively inhibit NRAS mutant melanoma in vitro and in vivo. Proc Natl Acad Sci U S A *110*, 4015-4020. 10.1073/pnas.1216013110.

Rambow, F., Marine, J.C., and Goding, C.R. (2019). Melanoma plasticity and phenotypic diversity: therapeutic barriers and opportunities. Genes Dev *33*, 1295-1318. 10.1101/gad.329771.119.

Rossi, M., Pellegrini, C., Cardelli, L., Ciciarelli, V., Di Nardo, L., and Fargnoli, M.C. (2019). Familial Melanoma: Diagnostic and Management Implications. Dermatol Pract Concept *9*, 10-16. 10.5826/dpc.0901a03.

Safina, D., Schlitt, F., Romeo, R., Pflanzner, T., Pietrzik, C.U., Narayanaswami, V., Edenhofer, F., and Faissner, A. (2016). Low-density lipoprotein receptor-related protein 1 is a novel modulator of radial glia stem cell proliferation, survival, and differentiation. Glia *64*, 1363-1380. 10.1002/glia.23009.

Saginala, K., Barsouk, A., Aluru, J.S., Rawla, P., and Barsouk, A. (2021). Epidemiology of Melanoma. Med Sci (Basel) *9*. 10.3390/medsci9040063.

Salah, D., Bohnet, K., Gueguen, R., Siest, G., and Visvikis, S. (1997). Combined effects of lipoprotein lipase and apolipoprotein E polymorphisms on lipid and lipoprotein levels in the Stanislas cohort. J Lipid Res *38*, 904-912.

Salama, Y., Lin, S.Y., Dhahri, D., Hattori, K., and Heissig, B. (2018). The fibrinolytic factor tPA drives LRP1-mediated melanoma growth and metastasis. FASEB J, fj201801339RRR. 10.1096/fj.201801339RRR.

Sanjana, N.E., Shalem, O., and Zhang, F. (2014). Improved vectors and genome-wide libraries for CRISPR screening. Nat Methods *11*, 783-784. 10.1038/nmeth.3047.
Schmidt, E.K., Clavarino, G., Ceppi, M., and Pierre, P. (2009). SUnSET, a nonradioactive method to monitor protein synthesis. Nat Methods *6*, 275-277. 10.1038/nmeth.1314.

Schneider, W.J., Kovanen, P.T., Brown, M.S., Goldstein, J.L., Utermann, G., Weber, W., Havel, R.J., Kotite, L., Kane, J.P., Innerarity, T.L., and Mahley, R.W. (1981). Familial dysbetalipoproteinemia. Abnormal binding of mutant apoprotein E to low density lipoprotein receptors of human fibroblasts and membranes from liver and adrenal of rats, rabbits, and cows. J Clin Invest *68*, 1075-1085. 10.1172/jci110330.

Soneson, C., Love, M.I., and Robinson, M.D. (2015). Differential analyses for RNA-seq: transcript-level estimates improve gene-level inferences. F1000Res *4*, 1521. 10.12688/f1000research.7563.2.

Song, H., Li, Y., Lee, J., Schwartz, A.L., and Bu, G. (2009). Low-density lipoprotein receptor-related protein 1 promotes cancer cell migration and invasion by inducing the expression of matrix metalloproteinases 2 and 9. Cancer Res *69*, 879-886. 10.1158/0008-5472.CAN-08-3379.

Spranger, S., Bao, R., and Gajewski, T.F. (2015). Melanoma-intrinsic beta-catenin signalling prevents anti-tumour immunity. Nature *523*, 231-235. 10.1038/nature14404.

Subramanian, A., Tamayo, P., Mootha, V.K., Mukherjee, S., Ebert, B.L., Gillette, M.A., Paulovich, A., Pomeroy, S.L., Golub, T.R., Lander, E.S., and Mesirov, J.P. (2005). Gene set enrichment analysis: a knowledge-based approach for interpreting genome-wide expression profiles. Proc Natl Acad Sci U S A *102*, 15545-15550. 10.1073/pnas.0506580102.

Sullivan, P.M., Mezdour, H., Aratani, Y., Knouff, C., Najib, J., Reddick, R.L., Quarfordt, S.H., and Maeda, N. (1997). Targeted replacement of the mouse apolipoprotein E gene with the common human APOE3 allele enhances diet-induced hypercholesterolemia and atherosclerosis. J Biol Chem *272*, 17972-17980. 10.1074/jbc.272.29.17972.

Sullivan, P.M., Mezdour, H., Quarfordt, S.H., and Maeda, N. (1998). Type III hyperlipoproteinemia and spontaneous atherosclerosis in mice resulting from gene replacement of mouse Apoe with human Apoe*2. J Clin Invest *102*, 130-135. 10.1172/JCI2673.

Suri, S., Heise, V., Trachtenberg, A.J., and Mackay, C.E. (2013). The forgotten APOE allele: a review of the evidence and suggested mechanisms for the protective effect of APOE varepsilon2. Neurosci Biobehav Rev *37*, 2878-2886. 10.1016/j.neubiorev.2013.10.010.

Surveillance Research Program, N.C.I. (2022). SEER*Explorer: An interactive website for SEER cancer statistics

Talmadge, J.E., and Fidler, I.J. (2010). AACR centennial series: the biology of cancer metastasis: historical perspective. Cancer Res *70*, 5649-5669. 10.1158/0008-5472.CAN-10-1040.

Tavazoie, M.F., Pollack, I., Tanqueco, R., Ostendorf, B.N., Reis, B.S., Gonsalves, F.C., Kurth, I., Andreu-Agullo, C., Derbyshire, M.L., Posada, J., et al. (2018). LXR/ApoE

Activation Restricts Innate Immune Suppression in Cancer. Cell *172*, 825-840 e818. 10.1016/j.cell.2017.12.026.

Truitt, M.L., and Ruggero, D. (2016). New frontiers in translational control of the cancer genome. Nat Rev Cancer *16*, 288-304. 10.1038/nrc.2016.27.

Turner, N., Ware, O., and Bosenberg, M. (2018). Genetics of metastasis: melanoma and other cancers. Clin Exp Metastasis *35*, 379-391. 10.1007/s10585-018-9893-y.

Van Gool, B., Dedieu, S., Emonard, H., and Roebroek, A.J. (2015). The Matricellular Receptor LRP1 Forms an Interface for Signaling and Endocytosis in Modulation of the Extracellular Tumor Environment. Front Pharmacol *6*, 271. 10.3389/fphar.2015.00271.

Vogelstein, B., Papadopoulos, N., Velculescu, V.E., Zhou, S., Diaz, L.A., Jr., and Kinzler, K.W. (2013). Cancer genome landscapes. Science *339*, 1546-1558. 10.1126/science.1235122.

Wang, B., Zhang, W., Zhang, G., Kwong, L., Lu, H., Tan, J., Sadek, N., Xiao, M., Zhang, J., Labrie, M., et al. (2021). Targeting mTOR signaling overcomes acquired resistance to combined BRAF and MEK inhibition in BRAF-mutant melanoma. Oncogene *40*, 5590-5599. 10.1038/s41388-021-01911-5.

Weisgraber, K.H., Innerarity, T.L., and Mahley, R.W. (1982). Abnormal lipoprotein receptor-binding activity of the human E apoprotein due to cysteine-arginine interchange at a single site. J Biol Chem *257*, 2518-2521.

Welch, H.G., Mazer, B.L., and Adamson, A.S. (2021). The Rapid Rise in Cutaneous Melanoma Diagnoses. N Engl J Med *384*, 72-79. 10.1056/NEJMsb2019760.

Westmark, P.R., Gutierrez, A., and Westmark, C.J. (2021). A Simple, Reliable and Inexpensive Method to Individually Identify Neonate Mice. Lab Animal Sci Prof *9*, 46-48.

Woldt, E., Matz, R.L., Terrand, J., Mlih, M., Gracia, C., Foppolo, S., Martin, S., Bruban, V., Ji, J., Velot, E., et al. (2011). Differential signaling by adaptor molecules LRP1 and ShcA regulates adipogenesis by the insulin-like growth factor-1 receptor. J Biol Chem *286*, 16775-16782. 10.1074/jbc.M110.212878.

Xu, Q., Bernardo, A., Walker, D., Kanegawa, T., Mahley, R.W., and Huang, Y. (2006). Profile and regulation of apolipoprotein E (ApoE) expression in the CNS in mice with targeting of green fluorescent protein gene to the ApoE locus. J Neurosci *26*, 4985-4994. 10.1523/JNEUROSCI.5476-05.2006.

Zivelin, A., Rosenberg, N., Peretz, H., Amit, Y., Kornbrot, N., and Seligsohn, U. (1997). Improved Method for Genotyping Apolipoprotein E Polymorphisms by a PCR-Based Assay Simultaneously Utilizing Two Distinct Restriction Enzymes. Clinical Chemistry *43*, 1657-1659. 10.1093/clinchem/43.9.1657.